Neutrino Masses from Cosmology: Cosmology Dependence and Systematic Biases

Aoife (“ee-feh”) Boyle

Institut d’Astrophysique de Paris

Collaborators: Fabian Schmidt, Eiichiro Komatsu, Sandrine Codis, Cora Uhlemann, Oliver Friedrich, Alexandre Barthelemy, Francis Bernardeau, Carlo Giocoli, Marco Baldi

Status

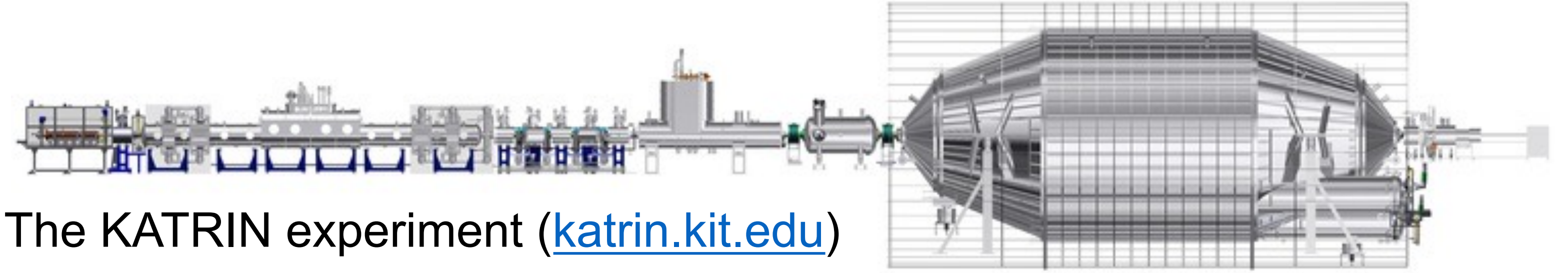

The KATRIN experiment (katrin.kit.edu)

Experiment	**Constrains**	**Constraints**
Solar / atmospheric oscillations	$\Delta m^2_{21}/\Delta m^2_{32}$	$M_\nu > 0.06$ eV
β decay	$m_{\nu,e}$	KATRIN aims for 90% C.L. constraint of **0.2 eV**
νless double β decay	$m_{\beta\beta}$ (requires Majorana nature)	Could reach KATRIN sensitivity (Dolinski+ 2019)
Cosmology	$M_\nu = \sum_{i=1}^{3} m_{\nu,i}$	Planck 2018 (TT, TE, EE, low E, CMB lensing, BAOs) $\boldsymbol{M_\nu < 0.12}$ **eV** (95% C.L.)!*

* Tension with DES clustering data increases the limit to 0.14 eV, internal inconsistencies related to the lensing amplitude have to be resolved, …

Motivation

$$F_{\alpha\beta} = \frac{\partial P_{gg}(k,\mu)}{\partial \theta_\alpha} C^{-1} \frac{\partial P_{gg}(k,\mu)}{\partial \theta_\alpha}$$

1. Cosmology dependence of constraints

Planck TT, TE, EE, lowE, lensing, BAOs

Cosmology	**M_ν (eV) upper bound (95% C.L.)**
ΛCDM+M_ν	0.12
$+ w_0$	0.19
$+ w_0 w_a$	0.25
$+ \Omega_k$	0.15
$+ A_L$	0.29

Table formed from results of Choudhury & Hannestad (2020)

2. "Deconstructing" constraints

Focus: Galaxy and CMB lensing power spectra

Distance Information → constrain $H(z), D_A(z)$

- BAOs
- Alcock-Paczynski test

Structure Growth Information

- Free-streaming causes small-scale suppression in power
- Change in amplitude (σ_8)
- RSDs → constrain $f(k)$

3. Degeneracies within ΛCDM

e.g. crucial degeneracy between M_ν and τ when combining CMB and LSS information

Motivation

$$F_{\alpha\beta} = \frac{\partial P_{gg}(k,\mu)}{\partial\theta_\alpha} \mathrm{C}^{-1} \frac{\partial P_{gg}(k,\mu)}{\partial\theta_\alpha}$$

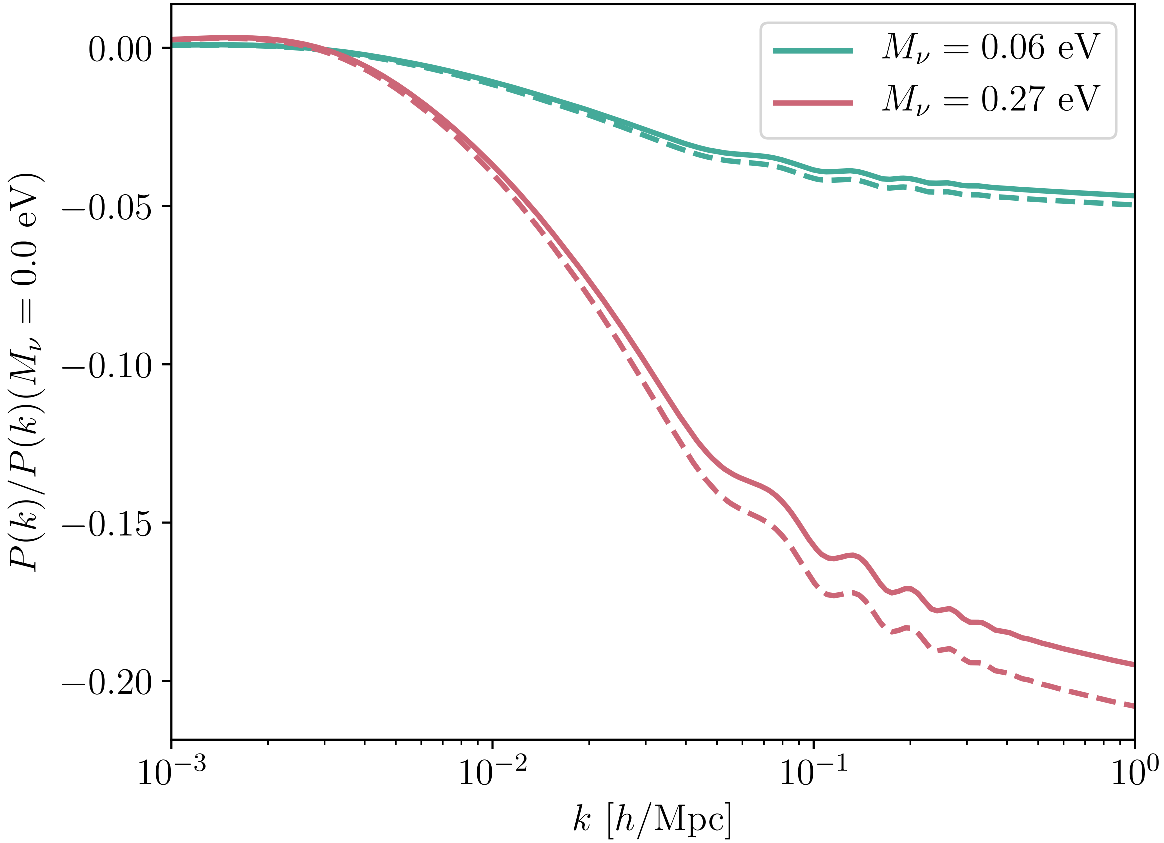

"Free-streaming" effect caused by relativistic → non-relativistic transition of neutrinos.

2. "Deconstructing" constraints

Focus: Galaxy and CMB lensing power spectra

Distance Information → constrain $H(z), D_A(z)$

- BAOs
- Alcock-Paczynski test

Structure Growth Information

- Free-streaming causes small-scale suppression in power
- Change in amplitude (σ_8)
- RSDs → constrain $f(k)$

3. Degeneracies within ΛCDM

e.g. crucial degeneracy between M_ν and τ when combining CMB and LSS information

Linear to NLO P(k)

Linear: $P_{gg}(k,\mu) = (b_1 + f_{bc}\mu^2)^2 P_{bc}(k) + n_g^{-1}$

NLO: Desjacques, Jeong & Schmidt, 2018 (1806.04015)

$$\delta_g(x,\tau) = \sum b_O(\tau) O(x,\tau) + \epsilon$$

Local bias expansion: $b_1\delta + \frac{1}{2}\boldsymbol{b_2}\delta^2 + \ldots$

Higher derivative bias: $\boldsymbol{b_{\nabla^2\delta}}\nabla^2\delta$

Tidal bias: $\boldsymbol{b_{K^2}}K^2 \rightarrow K^2 = K_{ij}K^{ij}$

$$\boldsymbol{b_{td}}O_{td} \rightarrow O_{td} = \frac{8}{21}K_{ij}D^{ij}\left(\delta_m^2 - \frac{3}{2}K^2\right)$$

Velocity bias: $\boldsymbol{b_{\nabla^2 v}}\nabla^2 v$

Stochastic parameters: $P_\epsilon^{\{0\}}, \boldsymbol{P_\epsilon^{\{2\}}}, \boldsymbol{P_{\epsilon\varepsilon_\eta}^{\{2\}}}$

Many of these parameters change the galaxy power spectrum in a scale-dependent way.

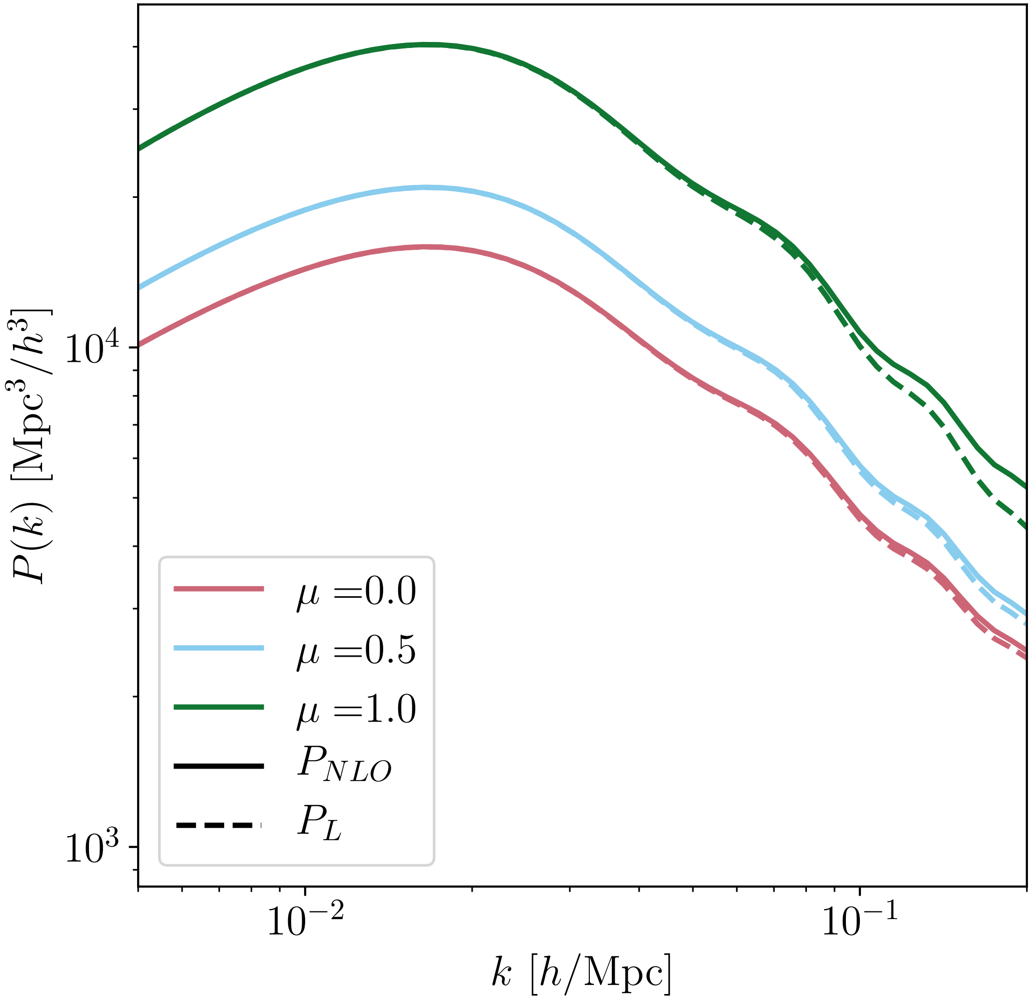

Change in the galaxy power spectrum at z=1.35.

Full Power Spectrum Constraints

Planck TT, Simons Observatory EE/TE, $\sigma(\tau) = 0.008$, Euclid $P_{gg}(k,\mu) \rightarrow 0.2\ h/\mathrm{Mpc}$.

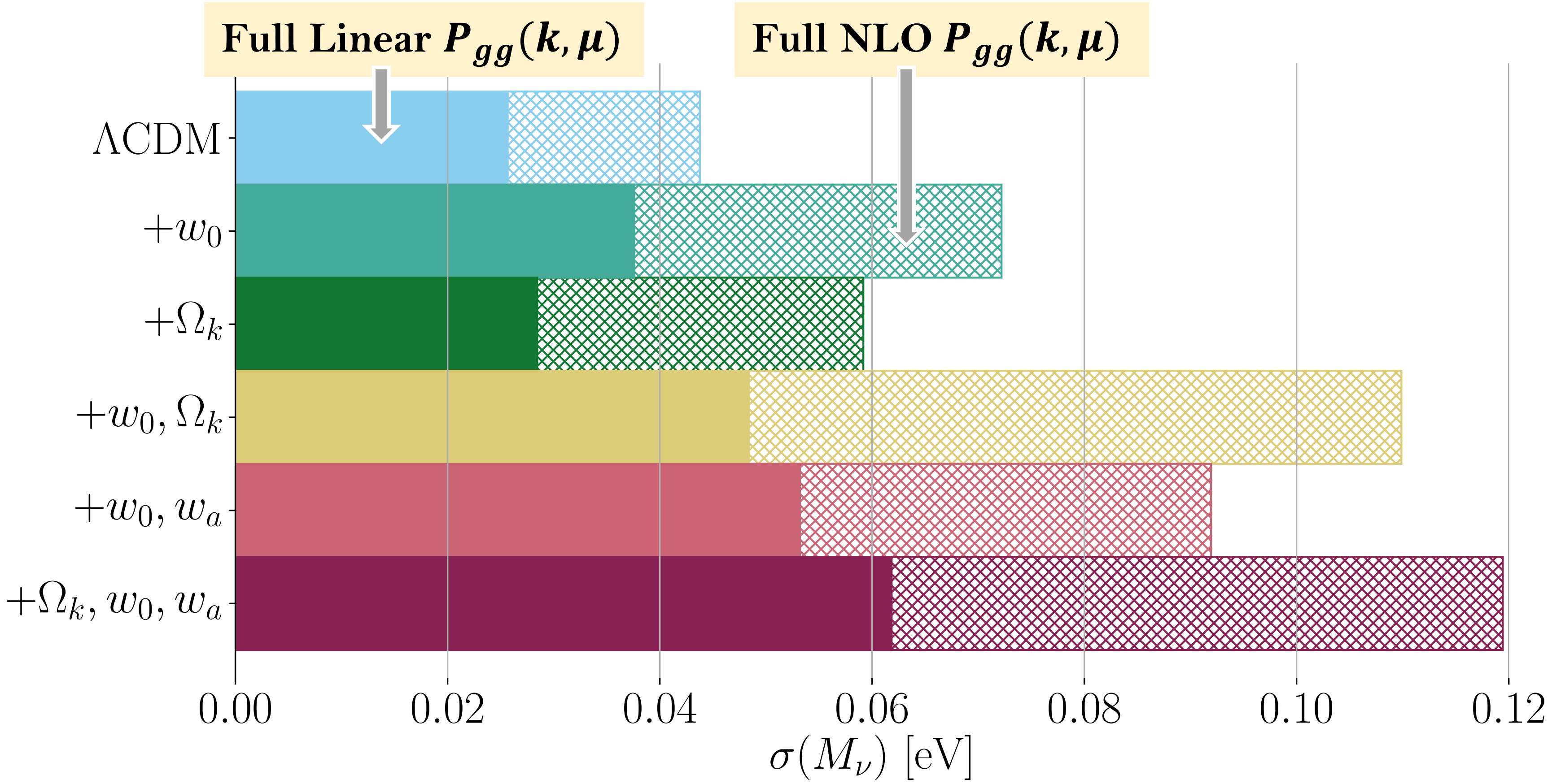

- New parameters degrade constraints significantly.
- Strong cosmology dependence.

$M_\nu - \tau$ Degeneracy (Linear GC Case)

Planck TT, Simons Observatory EE/TE, $\sigma(\tau) = 0.008$/Fixed, Euclid $P_{gg}(k,\mu) \rightarrow 0.2\ h$/Mpc.

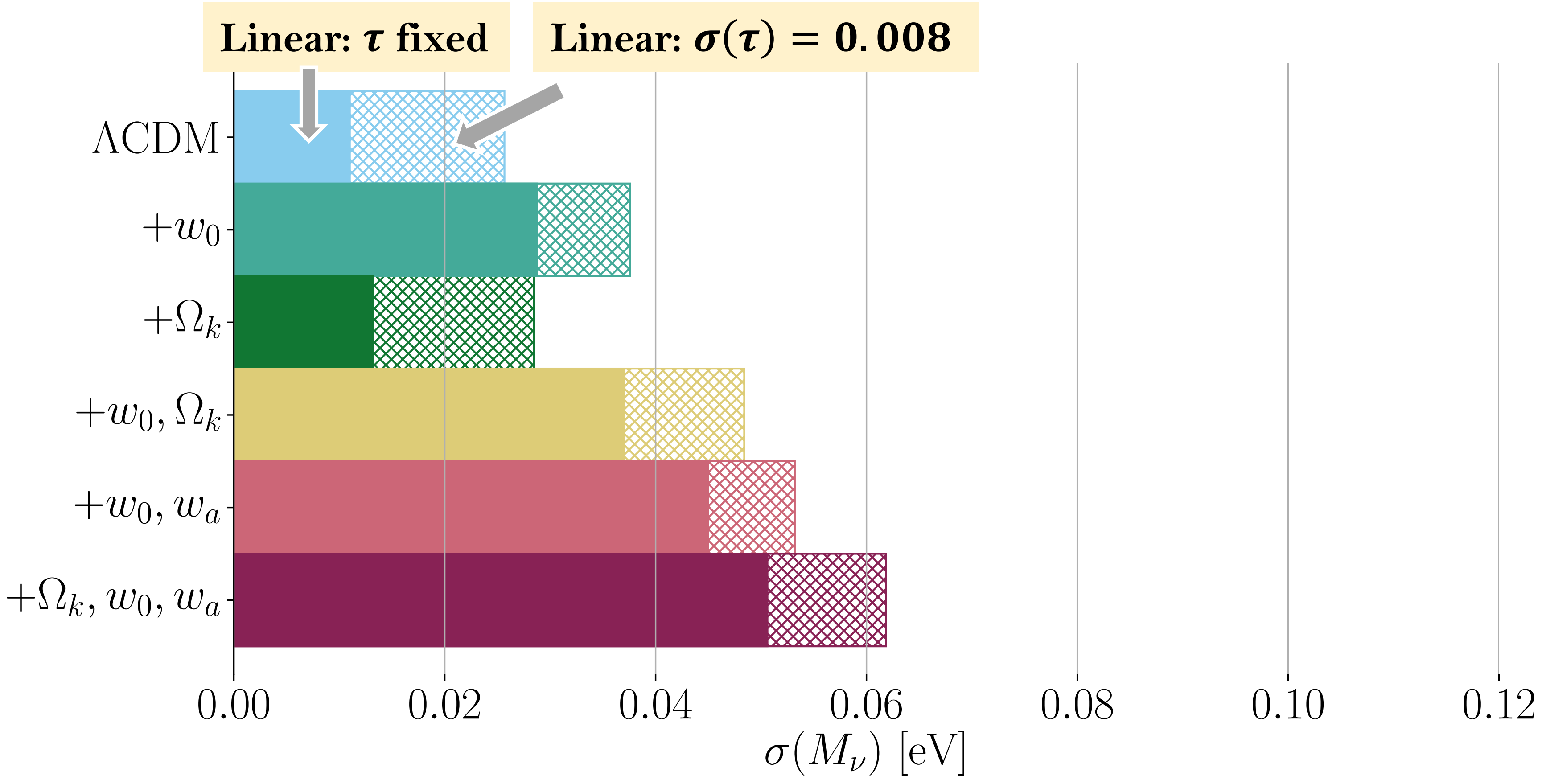

- Measure $A_s \exp(-2\tau)$ from CMB, $A_s \leftrightarrow M_\nu$ degeneracy in LSS measurements.
- In the linear case, τ degeneracy very significant.

$M_\nu - \tau$ Degeneracy (NLO GC Case)

Planck TT, Simons Observatory EE/TE, $\sigma(\tau) = 0.008$/Fixed, Euclid $P_{gg}(k,\mu) \rightarrow 0.2\ h$/Mpc.

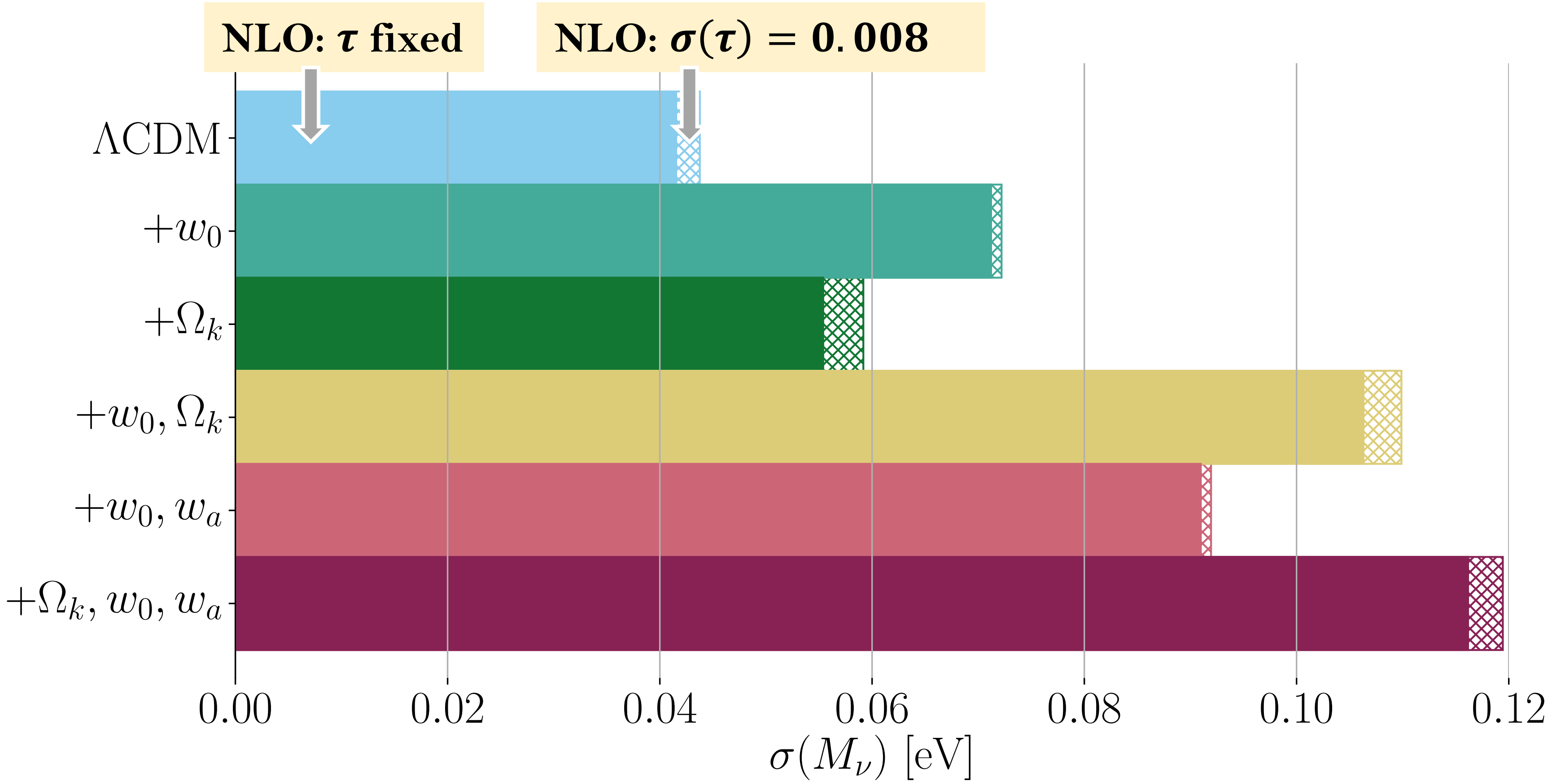

- τ degeneracy no longer relevant.
- Error supported by other degeneracies with new parameters:

$b_2, b_{\nabla^2\delta}, b_{K^2}, b_{td}, b_{\nabla^2 v}, P_\epsilon^{\{2\}}, P_{\epsilon\varepsilon_\eta}^{\{2\}}$

- The bias and stochastic parameters are primarily *all somewhat degenerate with each other*.

GC + CMB Lensing (NLO Case)

Planck TT, Simons Observatory EE/TE, $\sigma(\tau) = 0.008$, Euclid $P_{gg}(k, \mu) \rightarrow 0.2\ h$/Mpc, Simons Observatory $C_l^{\kappa\kappa}$

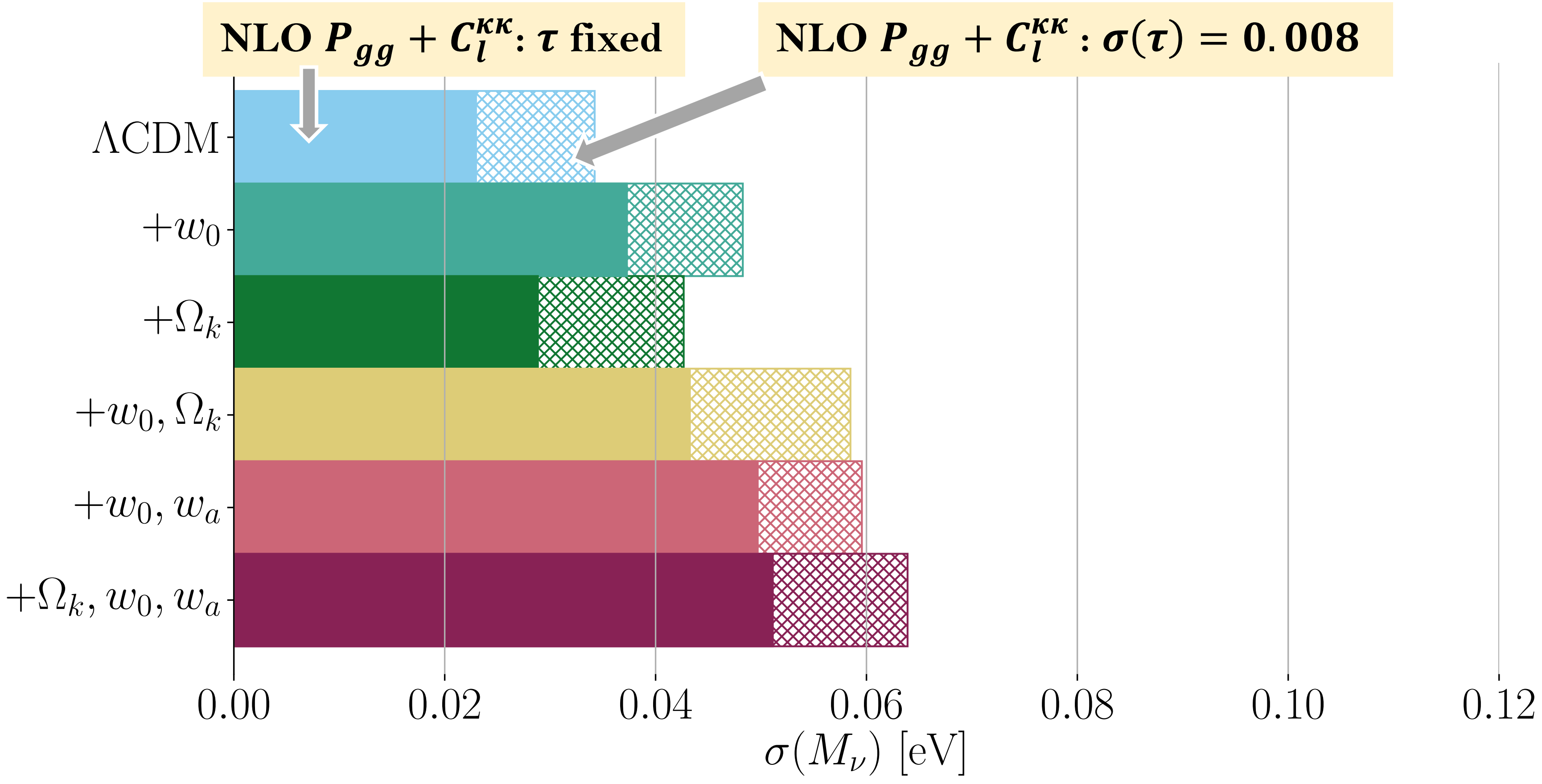

- CMB lensing significantly improves constraints.
- Keeps degeneracies with new bias parameters under control → τ degeneracy becomes important again.

Cosmology-Independent Constraints

- Isolating the relative suppression in power on small scales caused by massive neutrinos provides a cosmology-independent measurement of M_ν.
- This suppression is actually enhanced in the NLO case.

Where does this signature appear?

- $P_{mm}(z,k)$ (see plot) → $P_{gg}(z,k,\mu)$, $C_l^{\kappa\kappa}$, $C_l^{g\kappa}$ (latter is negligible)
- $f(z,k) \longrightarrow$ measured by RSDs

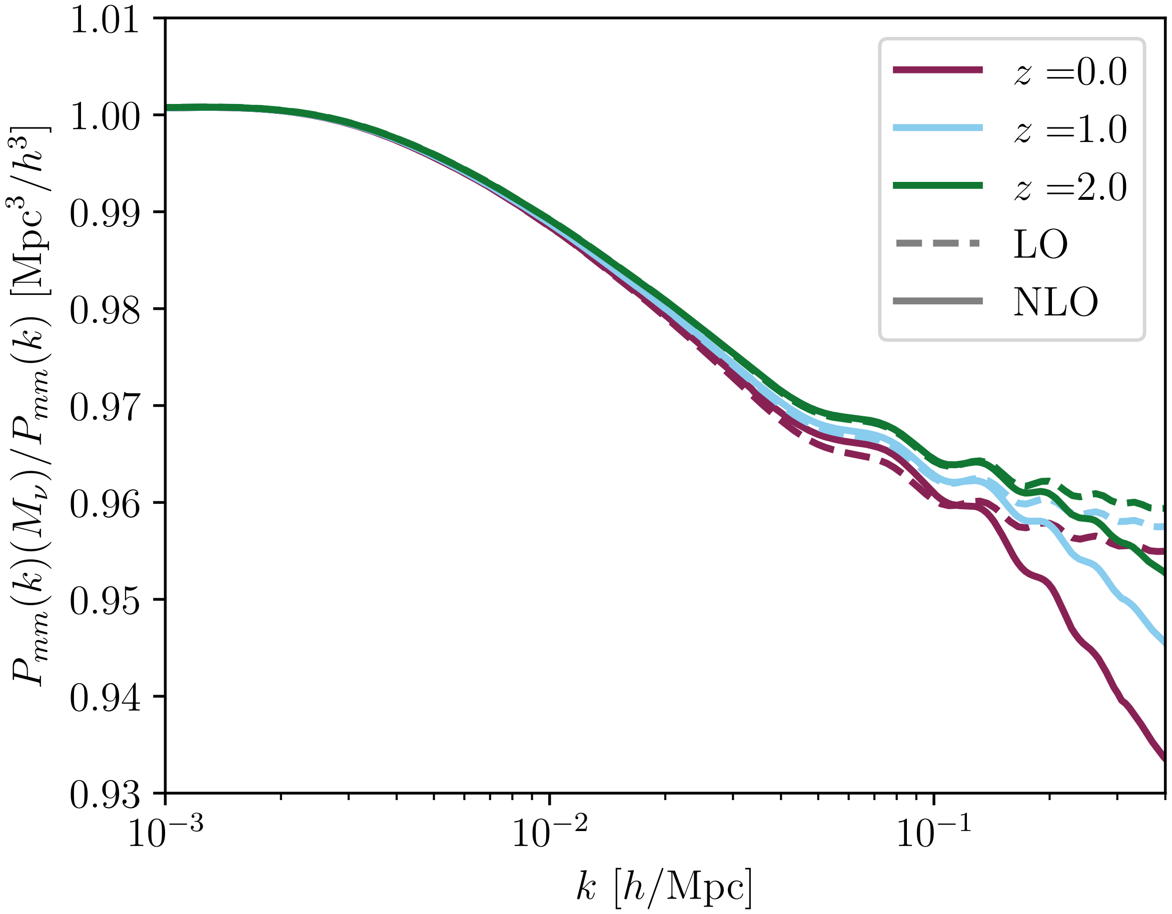

Cosmology-Independent Constraints

Planck TT, S.O. EE/TE, $\sigma(\tau) = 0.008$, Euclid P_{gg} (shape only) → 0.2 h/Mpc, S.O. $C_l^{\kappa\kappa}$ (shape only)

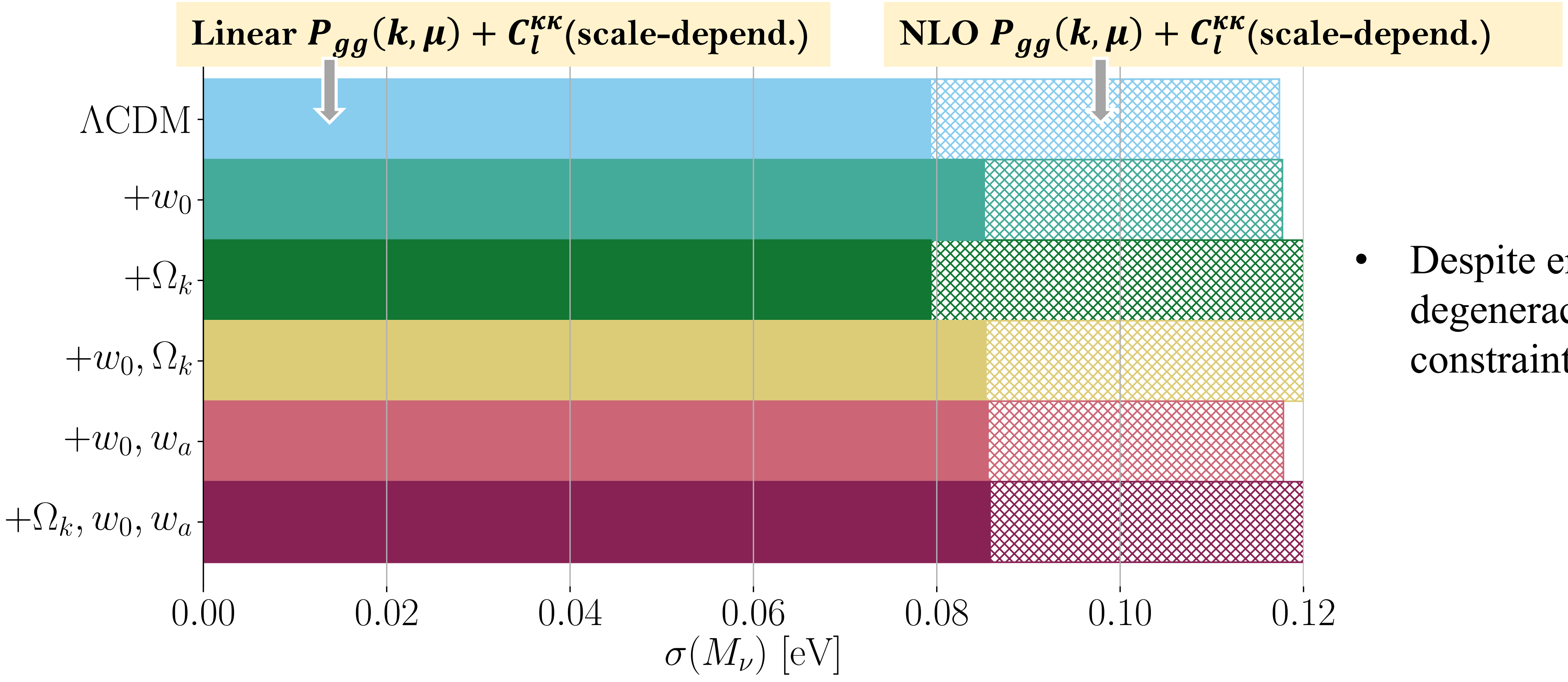

- Despite enhanced suppression, degeneracies weaken constraints.

Distance Measurements

$$P_{gg}(z,k,\mu) \to H(z), D_A(z) \to \{\theta\}$$

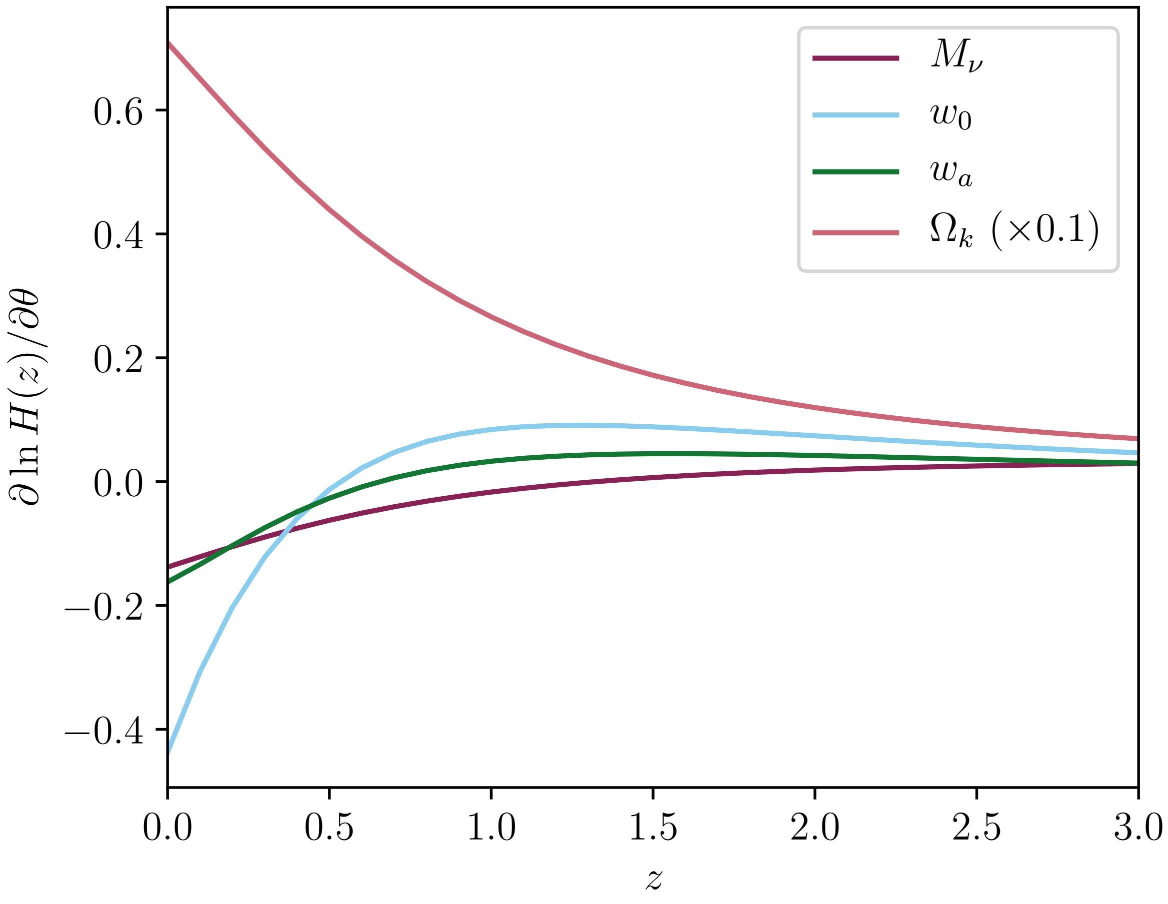

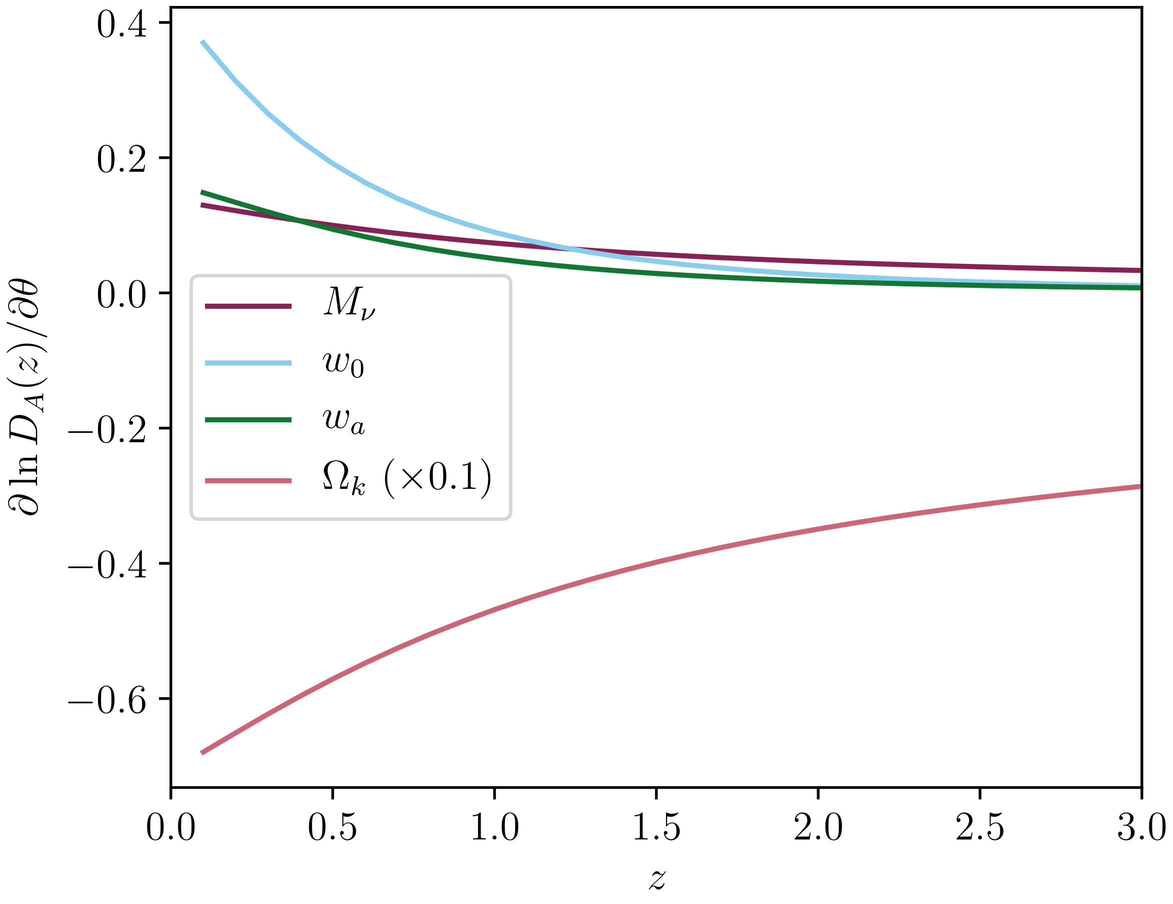

BAO-Only Constraints (Lin)

Planck TT, S. O. EE/TE, $\sigma(\tau) = 0.008$, Euclid BAOs only → 0.2 h/Mpc, S.O. $C_l^{\kappa\kappa}$

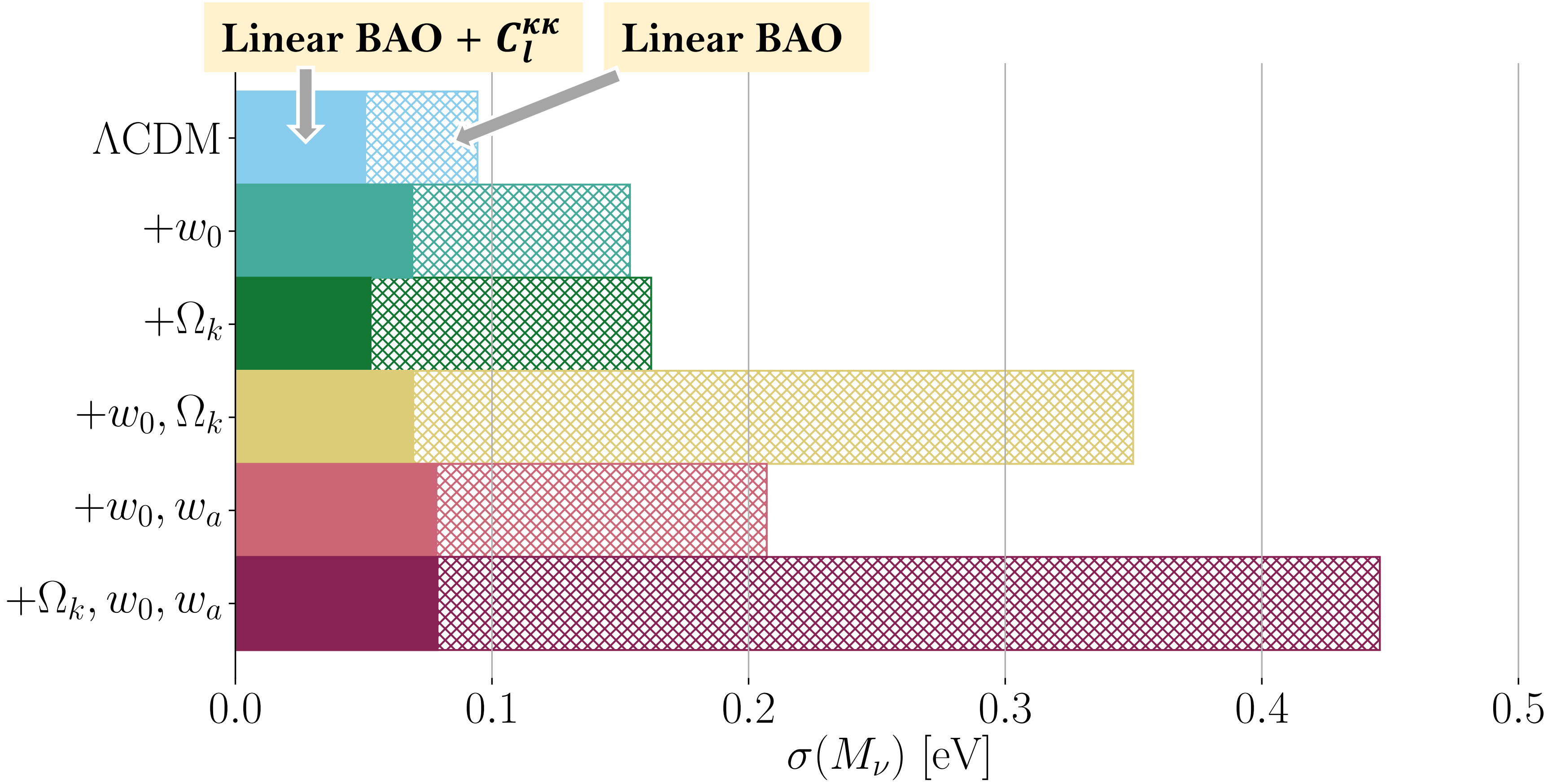

- Constraints from BAOs alone are very weak, particularly for extended cosmologies
- CMB lensing keeps Ω_k under control; still degeneracy with w

x-axis expanded by a factor ~5!!

BAO-Only Constraints + CMB Lensing (Lin)

Planck TT, S. O. EE/TE, $\sigma(\tau) = 0.008$, Euclid BAOs only $\rightarrow$ 0.2 h/Mpc, S.O. $C_l^{\kappa\kappa}$

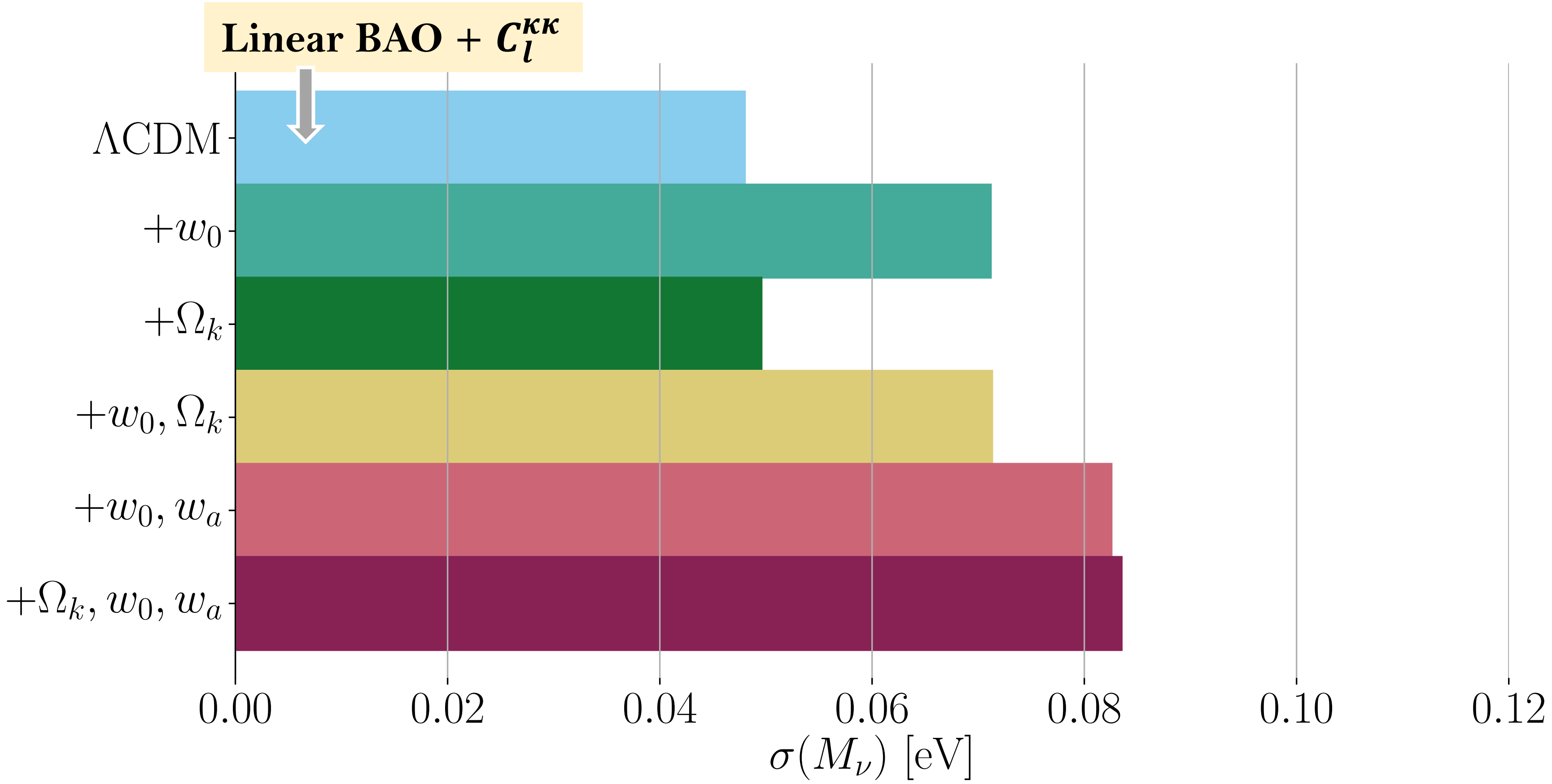

- Very little change between linear and NLO case
- CMB lensing keeps Ω_k under control; still degeneracy with w

Fisher Bias

Expand likelihood around true parameter values to derive systematic bias:

$$b[\theta_i] = \langle \theta_{\mathrm{sys},i} \rangle - \langle \bar{\theta}_i \rangle$$

$$= \sum_j (F^{-1})_{ij} \sum_x \frac{\overbrace{O^{\mathrm{sys}}(x)}^{\text{e.g. } P_{gg,lin}(k,\mu) - P_{gg,NLO}(k,\mu)}}{Var[\hat{O}(x)]} \frac{\partial O^{\mathrm{theory}}(x)}{\partial \theta_j}$$

(other components all from original Fisher calculation)

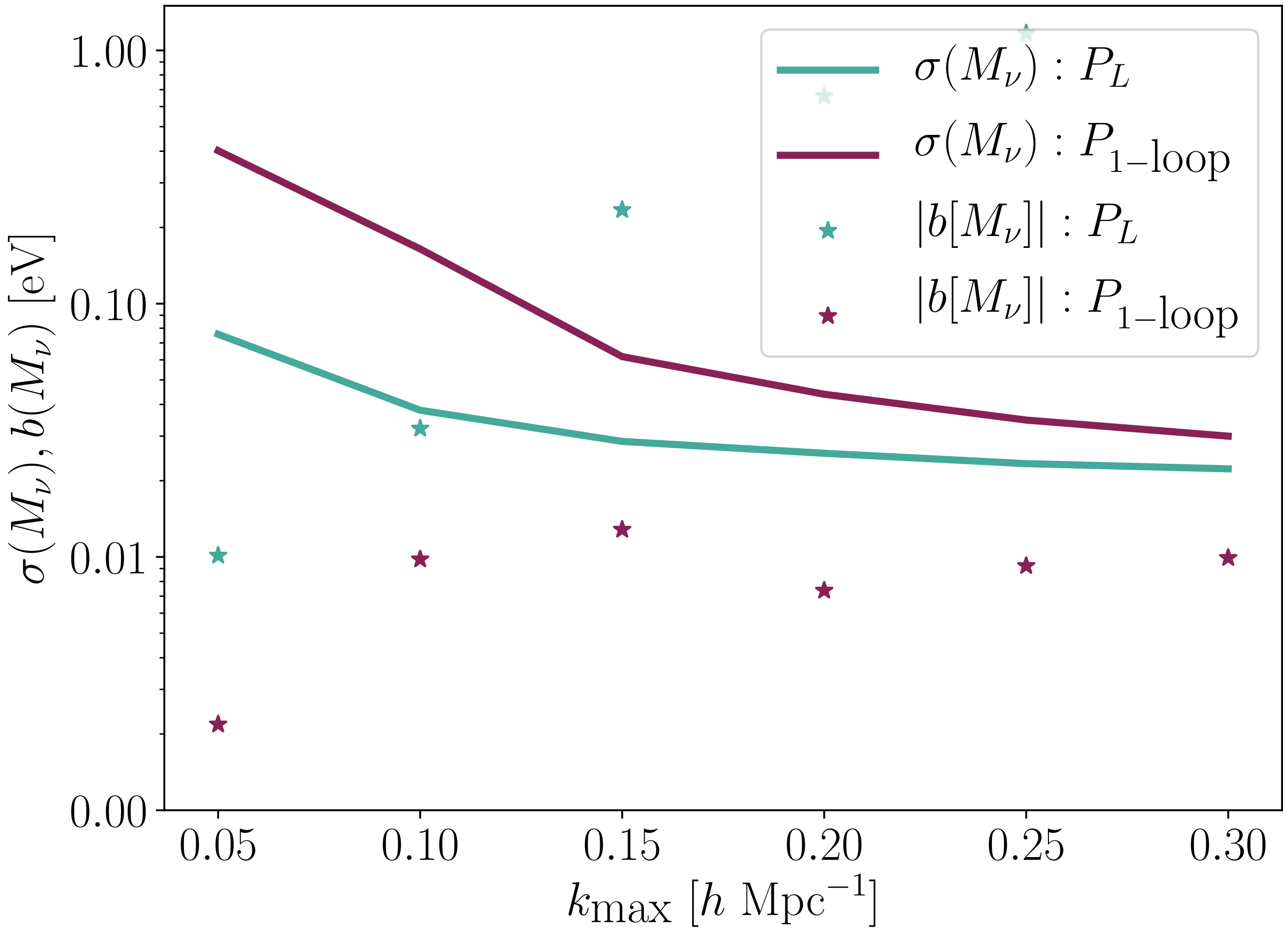

Fisher Bias

Don't have a full expression for $P_{gg,2-loop}$.

Assume
$P_{gg,2-loop}(k,\mu)$
$\approx (b_1 + f(k)\mu^2)^2 P_{mm,2-loop}(k)$

- Linear bias: exceeds constraint from $k_{max} = 0.1\ h$/Mpc.
- 1-loop bias (estimate): bias approximately 20% of constraint at $k_{max} = 0.2\ h$/Mpc.

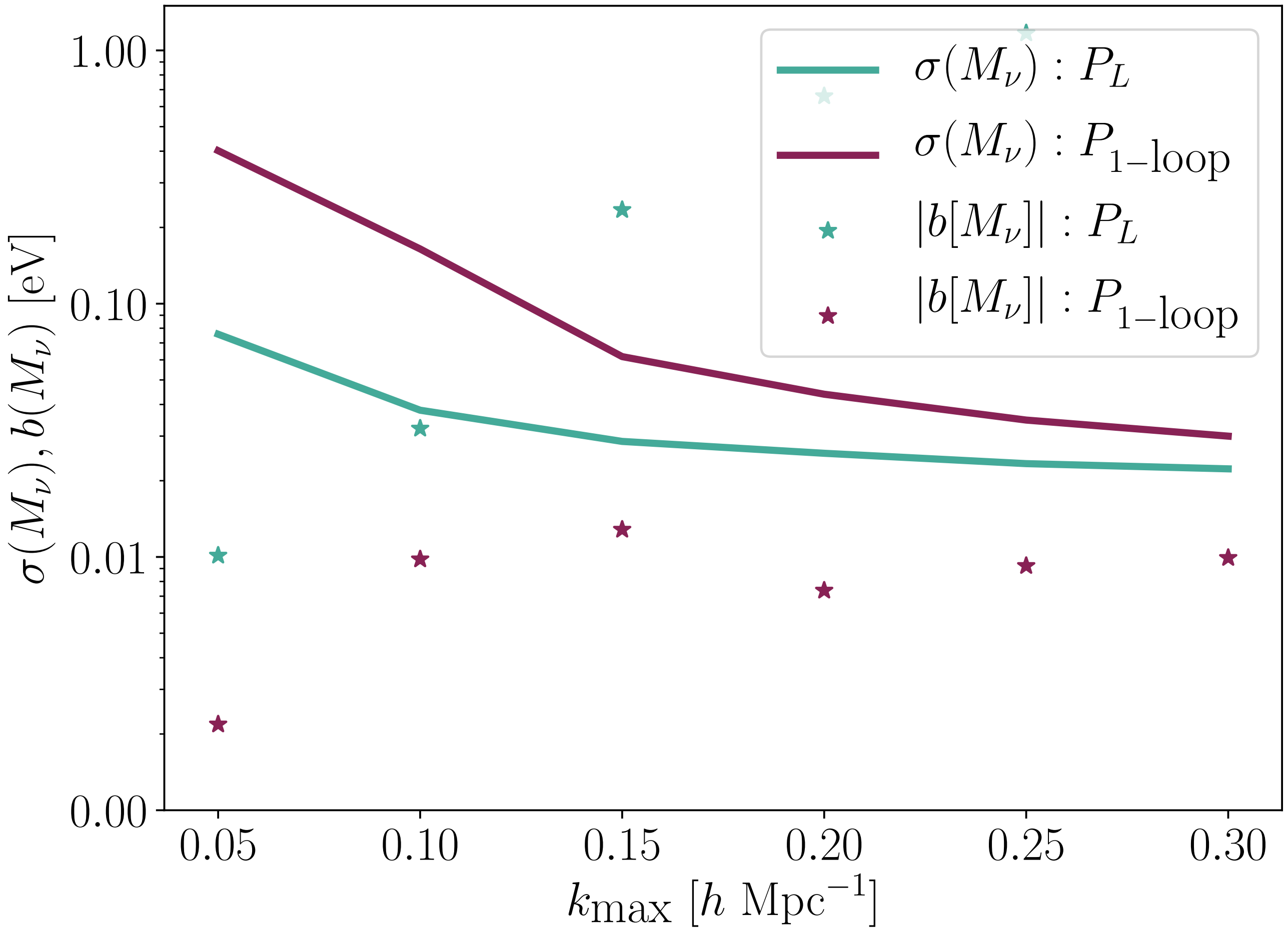

Conclusions (Part 1)

Considering the 1-loop power spectrum has a significant qualitative and quantitative impact on neutrino mass constraints.

- 7 new free parameters → constraints degrade considerably. **Realistic constraints, even up to k=0.2 h/Mpc, should include these parameters.**
- CMB lensing can play a significant role in keeping effects of degeneracies with additional nuisance parameters under control.
- Free-streaming constraints remain cosmology-independent, though weaker.
- The 1-loop power spectrum seems reasonably unbiased compared to the linear power spectrum.

Neutrino mass constraints (apart from the free-streaming only constraints we developed) are strongly cosmology dependent.

AB, C. Uhlemann, O. Friedrich, A. Barthelemy, S. Codis, F. Bernardeau++, 2012.07771

Introduction (Part 2)

- Theoretical model for the WL convergence PDF from Barthelemy et al. (2020).
- Validate cosmology-dependence of model with simulations.
- Apply model to predict constraining power of convergence PDF.

Why the PDF? Easy to measure, complementary to power spectrum.

Why a theoretical model? Physical intuition, avoids simulation expense.

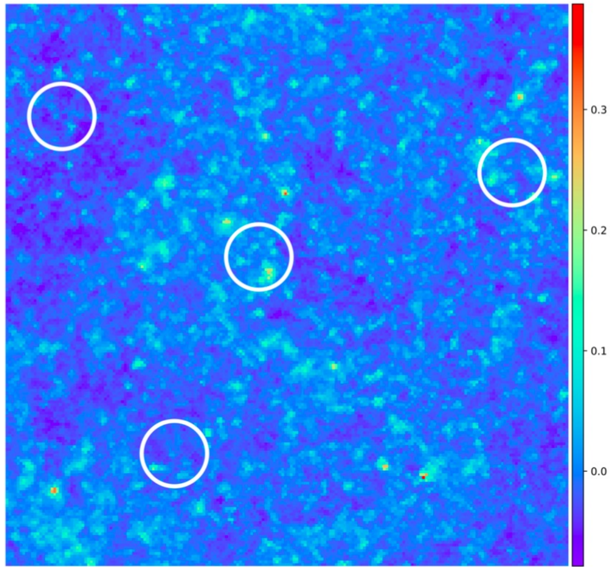

Barthelemy et al. (2020)

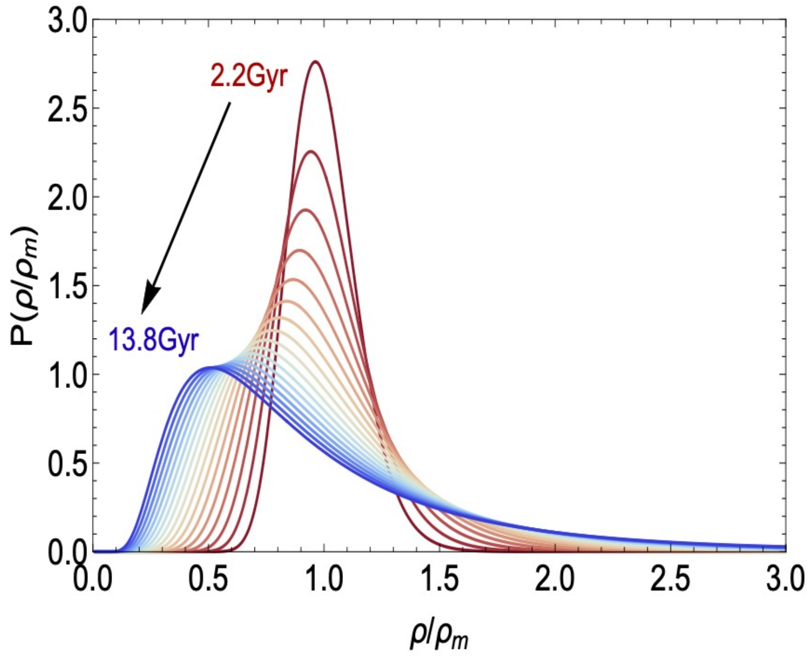

Large Deviation Statistics

- For LDT variable δ, the log PDF is characterised by the rate function, Ψ. Under Gaussian initial conditions:

$$P_r^{initial}(\delta_L) \sim \exp\left[-\frac{\boldsymbol{\delta_L^2}}{\boldsymbol{2\sigma_L^2(r)}}\right]$$

- Beauty of LDT: the *contraction principle*.

$$\boldsymbol{\Psi^{initial}} \xrightarrow{\textbf{spherical collapse}} \boldsymbol{\Psi^{final}}$$

$$P_r^{later}(\rho) \sim \exp\left[-\frac{\boldsymbol{\delta_L^2(\rho)}}{2\sigma_L^2(z, r_{initial}(R,\rho))}\frac{\boldsymbol{\sigma_L^2}}{\boldsymbol{\sigma_{NL}^2}}\right]$$

- One non-analytical ingredient → we rescale by the non-linear variance (from Halofit).

Matter Density Results

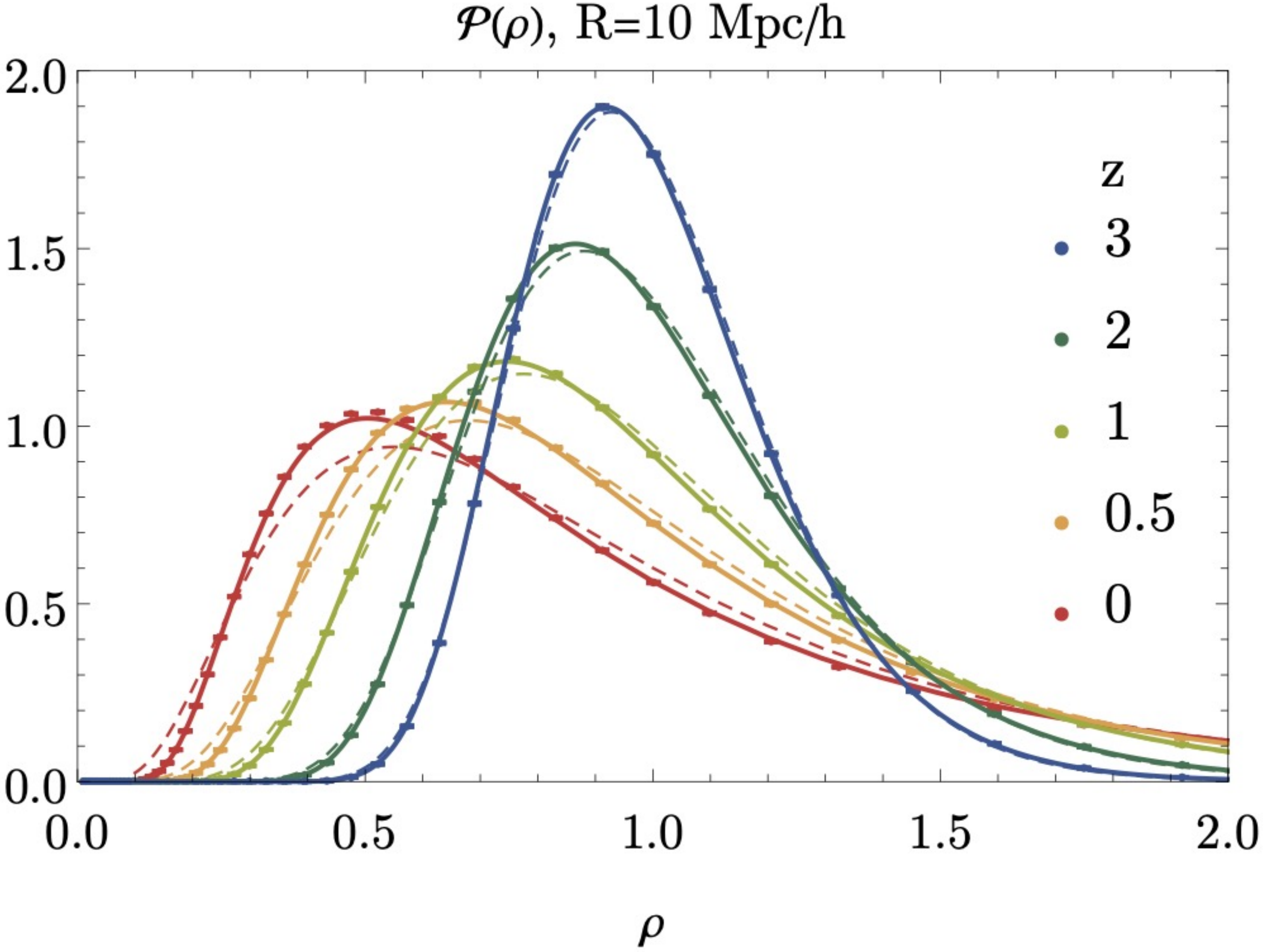

Uhlemann et al. (2020): Matter PDFs smoothed in spheres.

Dots from **Quijote** simulations, solid lines from LDT prediction, dashed lines lognormal fit.

LDT provides percent-level accurate PDFs analytically on scales beyond the reach of perturbation theory!

Applying Large Deviation Theory to Weak Lensing

- Apply LDT to slices of a cone → apply cylindrical instead of spherical collapse. Work in terms of the cumulant generating function ϕ:

$$\phi_{\kappa,\theta}(y) = \int_0^{z_s} dz\, R'(z)\, \phi_{\delta,cyl}(\omega(z,z_s)y, d_A(z)\theta, z)$$

- Barthelemy et al. (2020) showed the model can replicate the WL PDF from simulations very accurately.
- In Boyle et al. (2020) we show the PDF responds accurately to changes in cosmology, and perform a Fisher forecast.

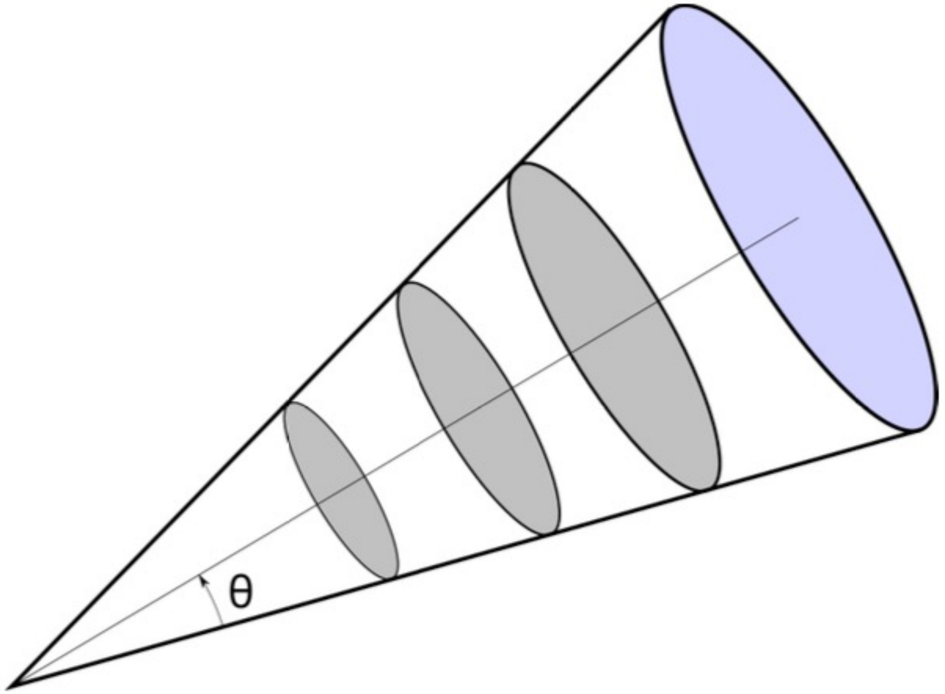

Barthelemy et al. (2020)

Simulations and Calculation Details

TAKAHASHI Takahashi et al. (2017):

- Full-sky, 108 realisations, single cosmology

DUSTGRAIN-COSMO Giocoli et al. (2018):

- 256 maps of 25 deg^2 for a fiducial cosmology and variations of Ω_{cdm}, σ_8 and w.

MASSIVENUS Liu et al. (2018):

- 10,000 maps of 12.25 deg^2 for a fiducial cosmology with and without massive neutrinos

- Fisher matrix approach
- Single source redshift: $z_s = 2$
- Euclid-like survey: 15,000 deg^2
- n_g = 30 arcmin^{-2} / 8 arcmin^{-2}
- Two top-hat smoothing scales: $\theta = 7.32'$, $10.25'$

Validating the Theory: Fiducial Cosmology

Compared to TAKAHASHI (full-sky) simulations, with σ^2_{NL} from Halofit.

Bins used

2% accuracy in range we consider

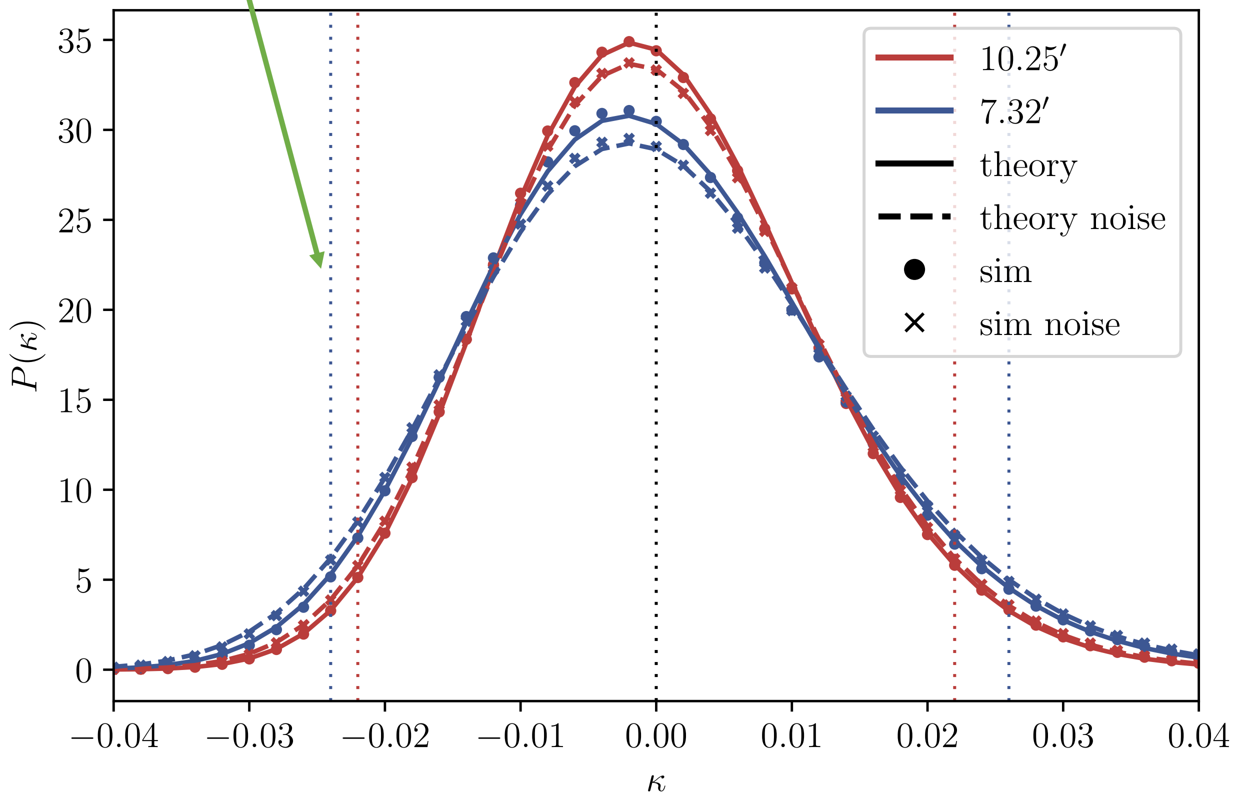

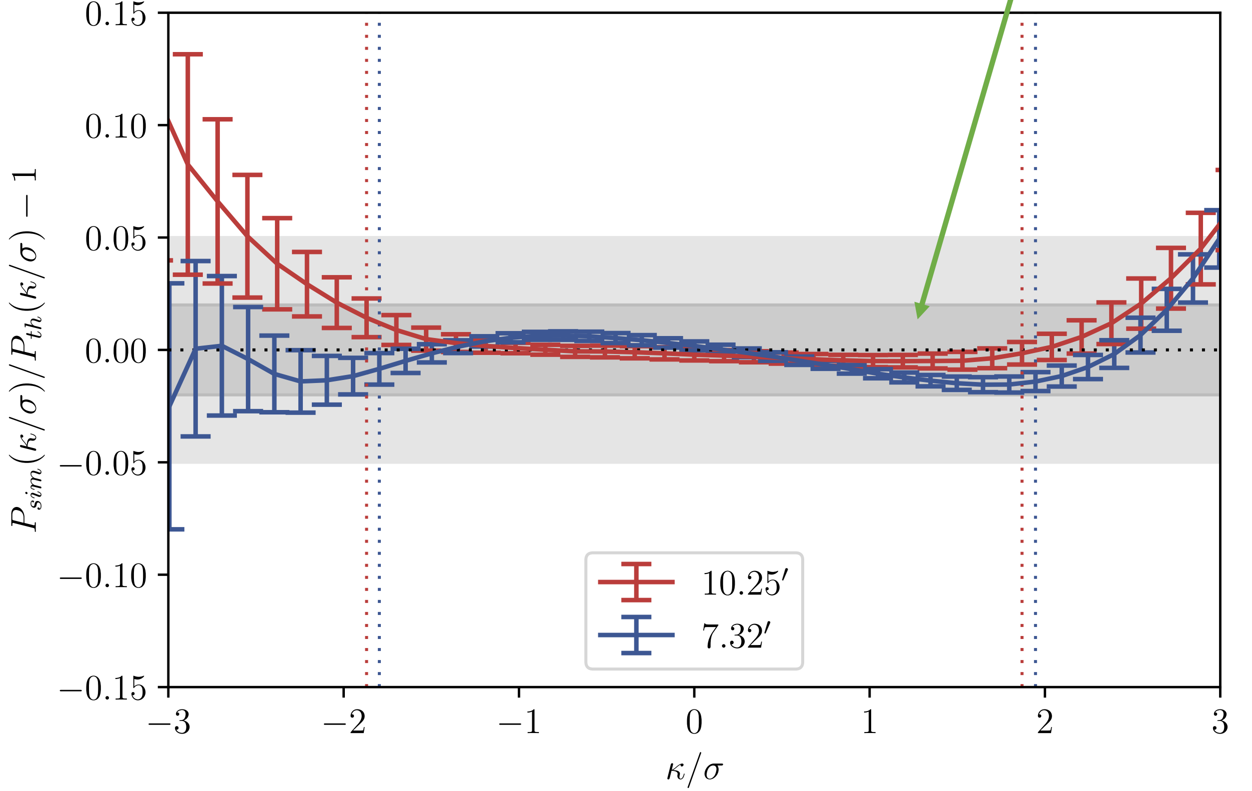

Validation: Derivatives for Ω_{cdm}, σ_8 and w

Compared to DUSTGRAIN simulations. σ_{NL}^2 must include cut in l to account for small patch size.

Extrema differ despite similar shapes

Theoretical result only for fiducial DUSTGRAIN cosmology + M_ν (validated next slide with MASSIVENUS)

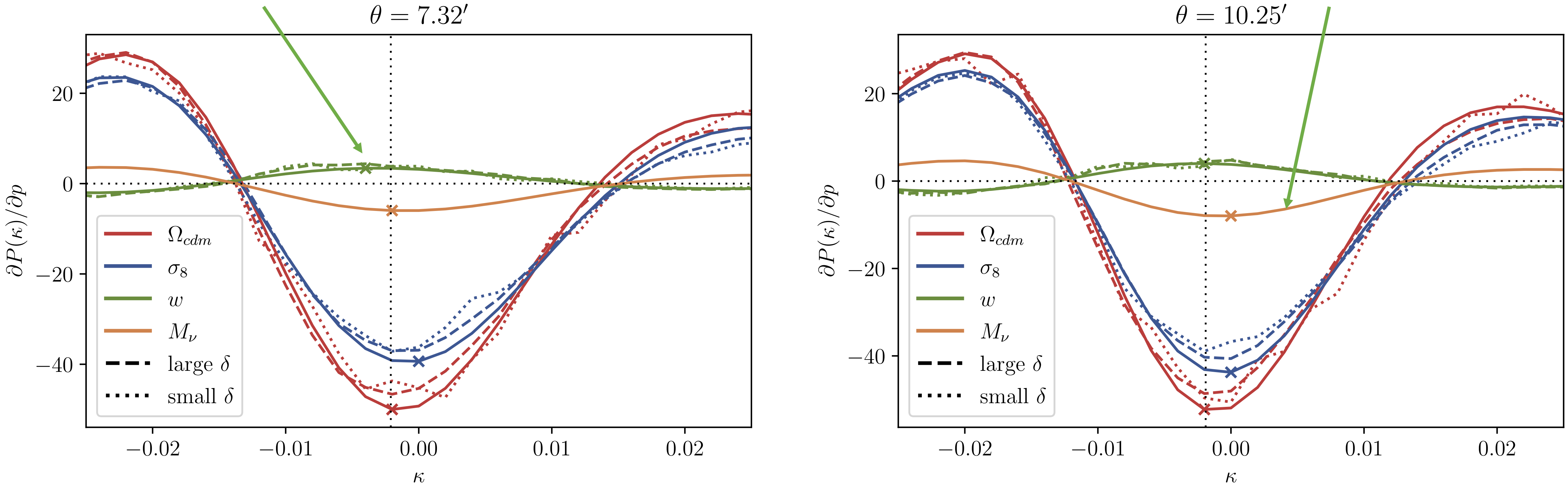

Validation: Derivatives for M_ν

Compared to MassiveNuS simulations.

Sparsely dotted lines show theoretical results without massive neutrinos but with σ_8 rescaled to match that when M_ν is included → extremely similar.

Expect strong $\boldsymbol{\sigma_8 - M_\nu}$ degeneracy.

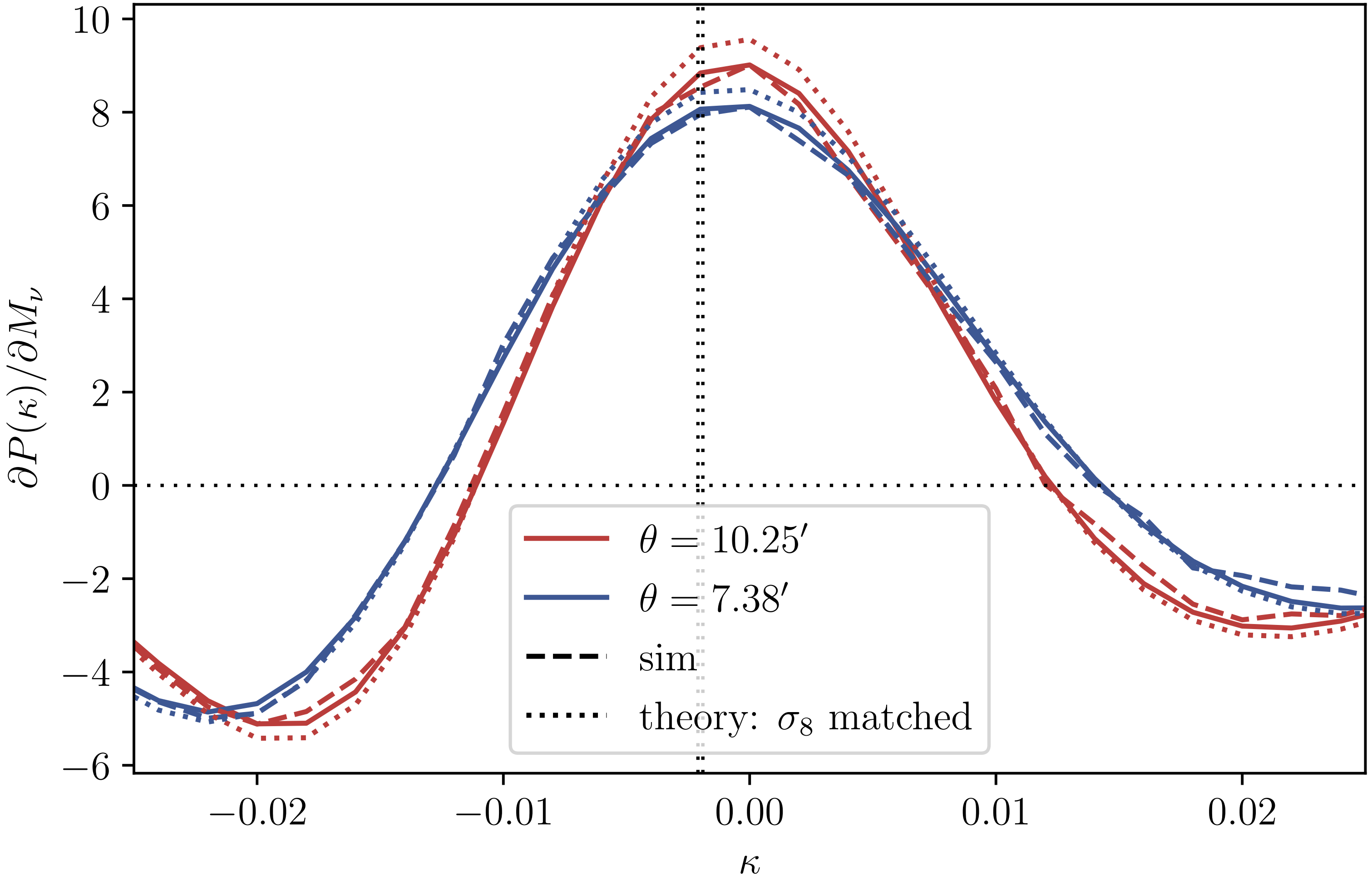

arXiv: 2011.10594, 2012.07771

Covariance Matrix

$$F_{\alpha\beta} = \frac{\partial P}{\partial \theta_\alpha} \mathrm{C}^{-1} \frac{\partial P}{\partial \theta_\beta}$$

- Use FLASK (Xavier at al., 2016) to efficiently generate 500 convergence maps.
- Assumes the convergence field has a shifted lognormal distribution.
- Requires an input power spectrum and shift parameter (set to reproduce the theoretical skewness).
- Excellent agreement with covariance matrix from DUSTGRAIN.

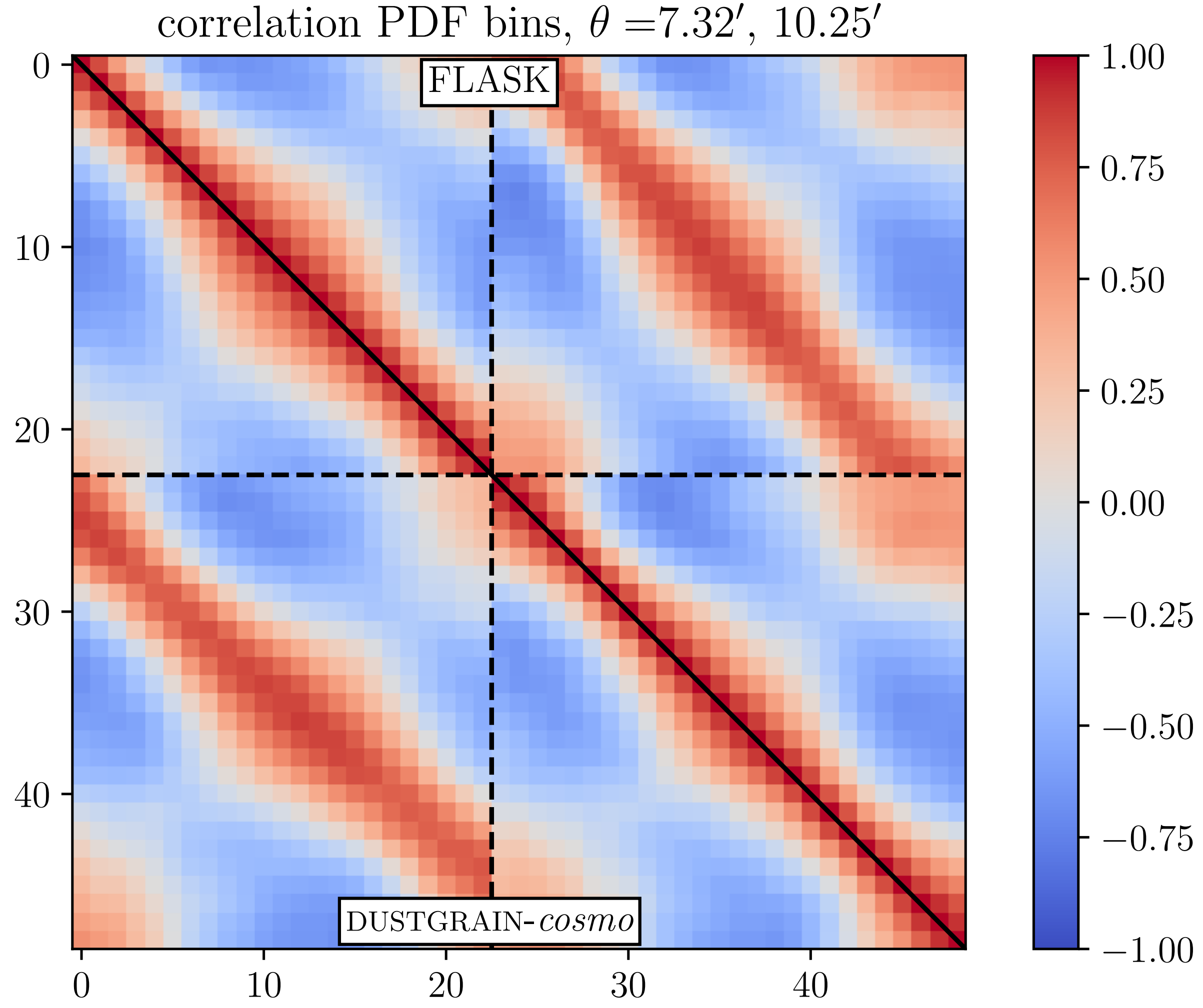

arXiv: 2011.10594, 2012.07771

Results

All results for theoretical derivatives and FLASK covariances.

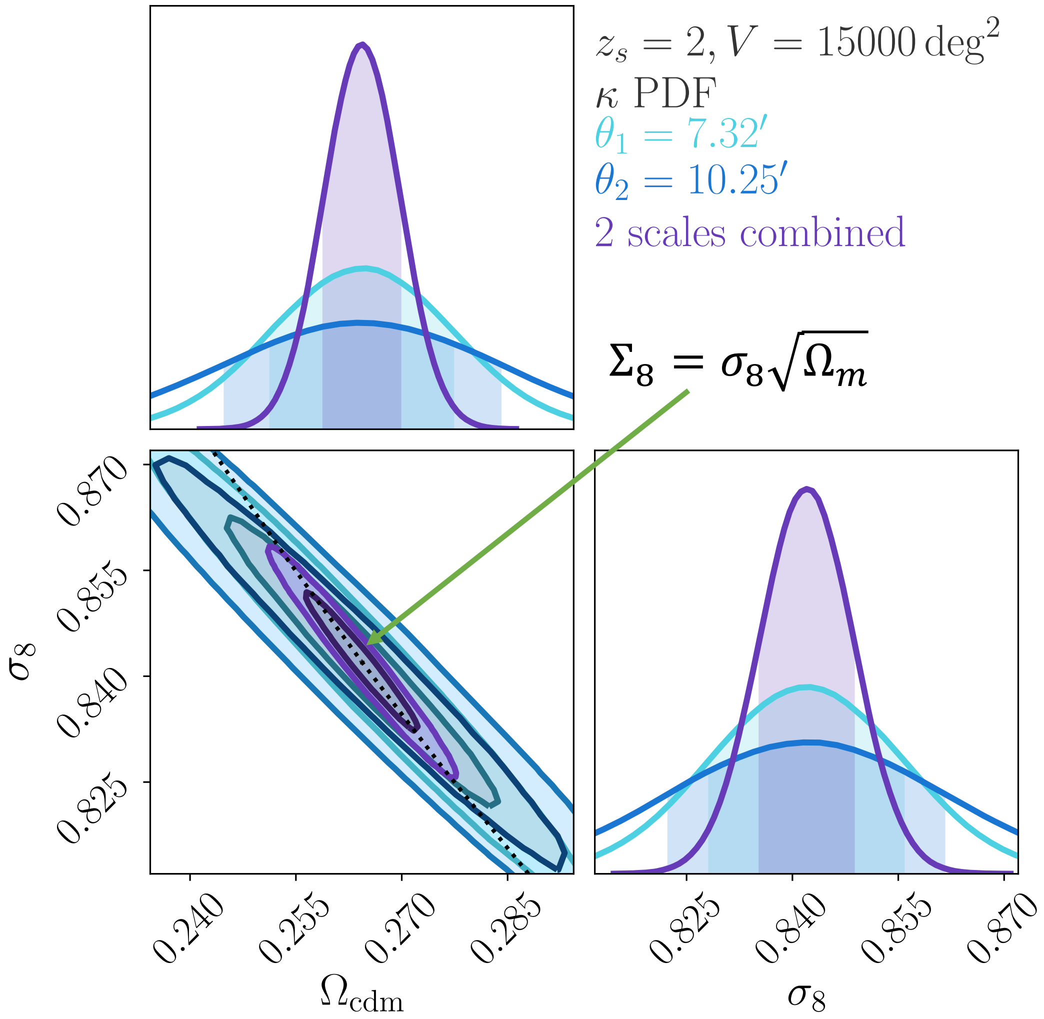

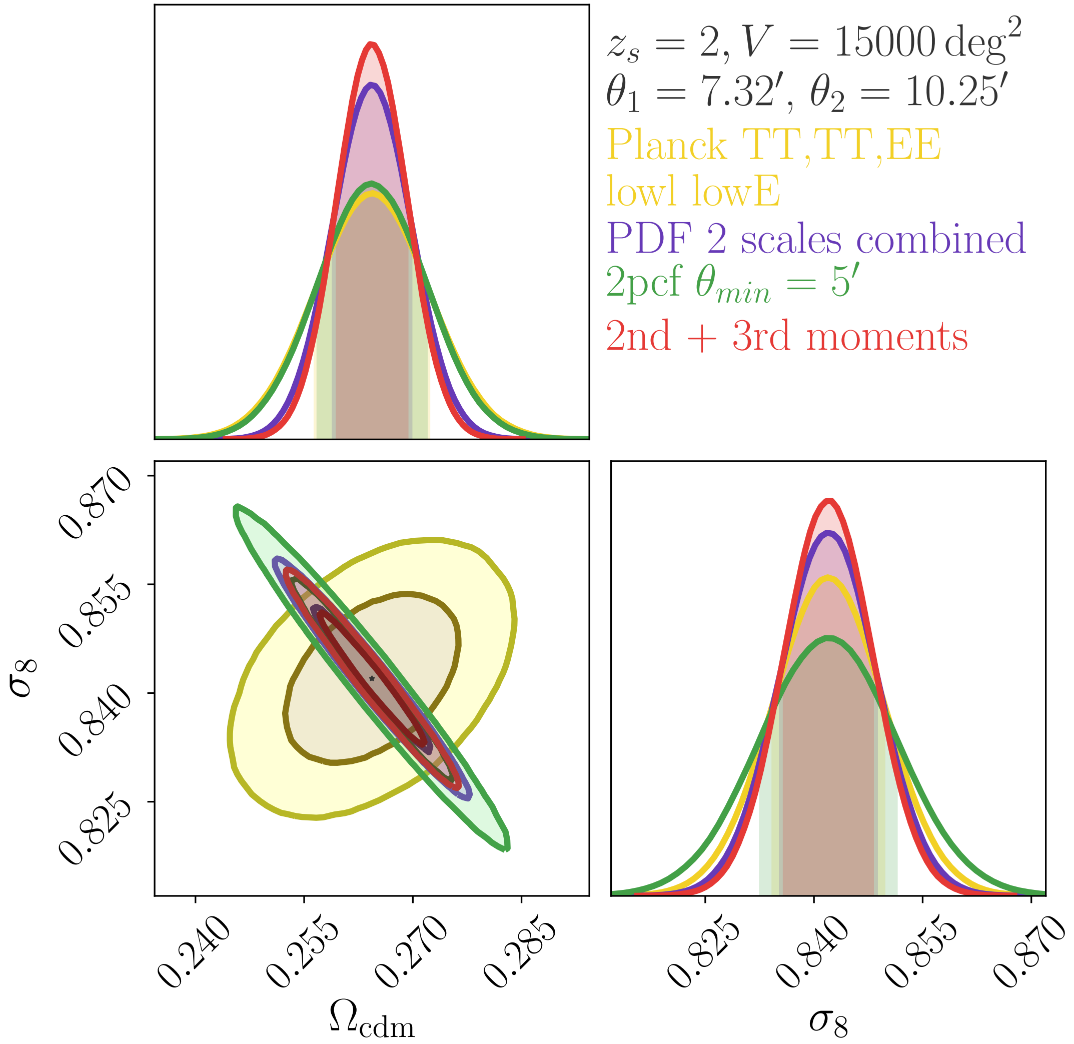

PDF vs. Moments

The values of the lowest and highest PDF bins we use show clear Gaussian distribution.

The second and third moments **do not** → not optimal for Fisher matrix calculations.

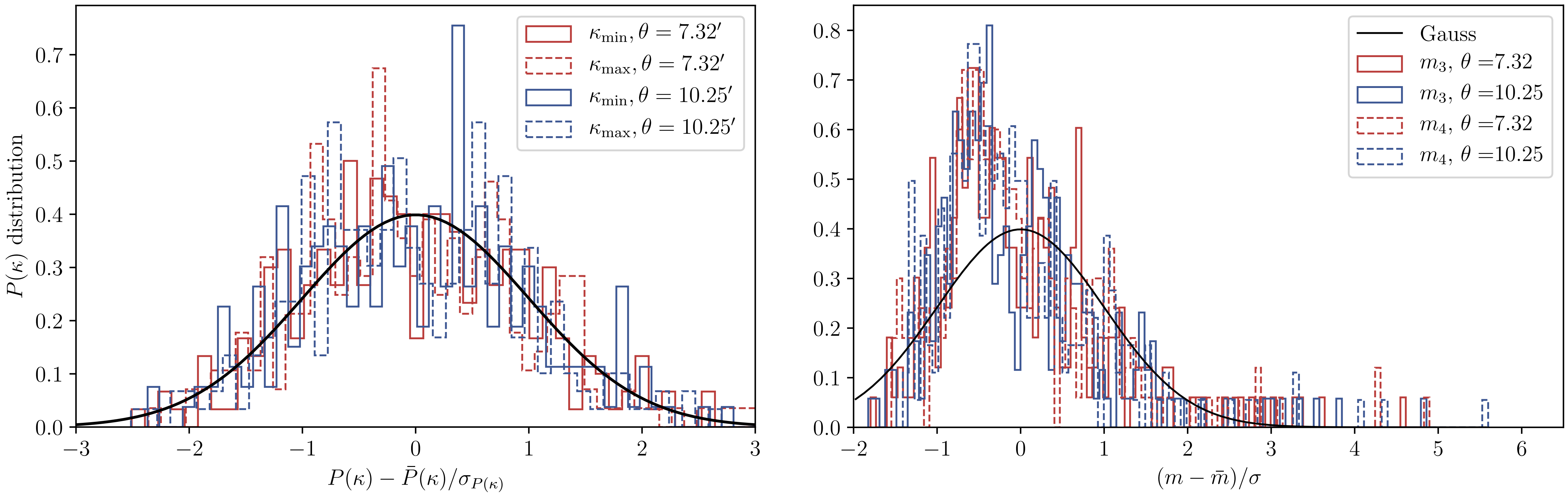

Results

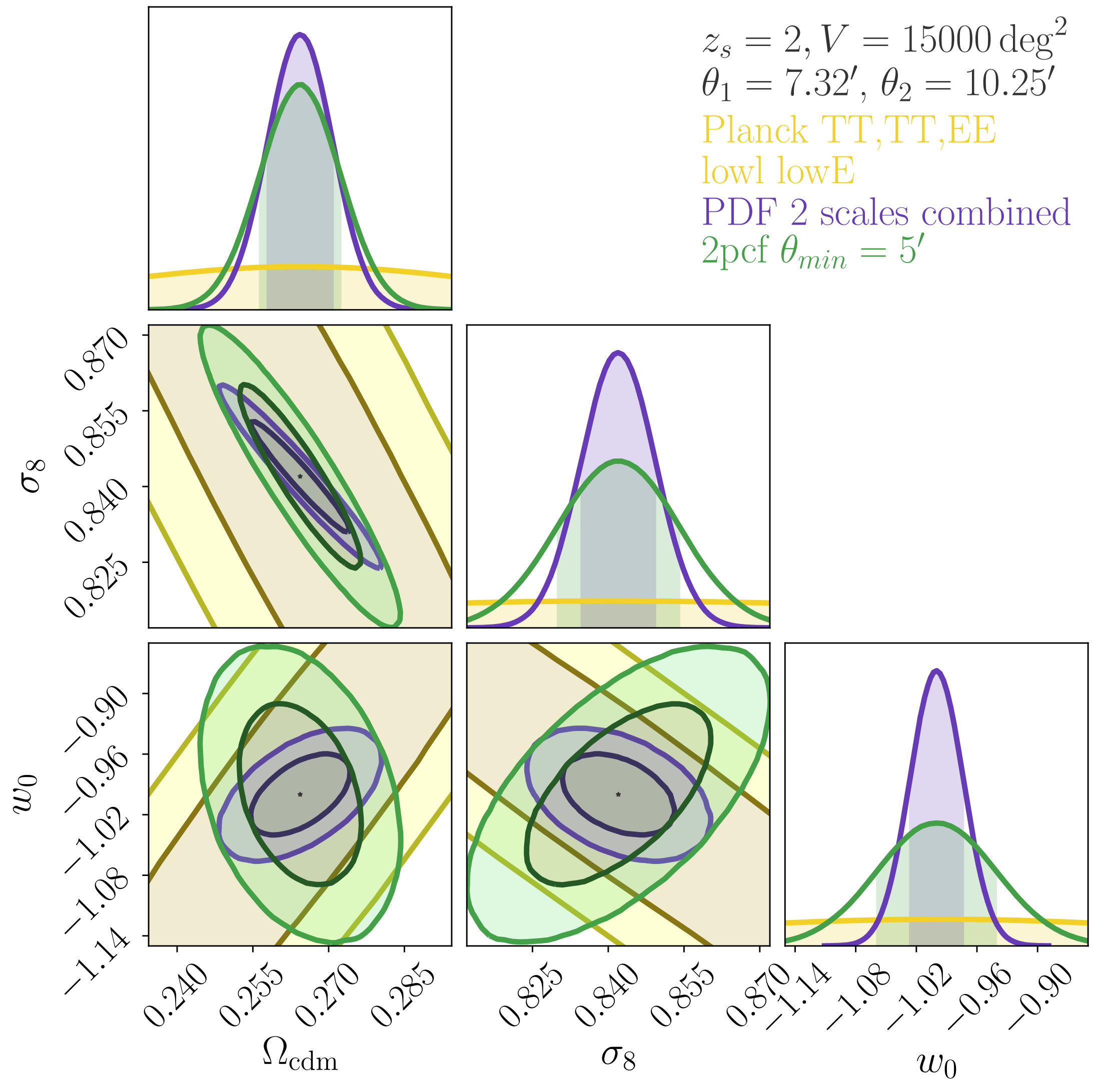
$z_s = 2, V = 15000\,\mathrm{deg}^2$
$\theta_1 = 7.32', \theta_2 = 10.25'$
Planck TT,TT,EE
lowl lowE
PDF 2 scales combined
2pcf $\theta_{min} = 5'$
σ_8
w_0
$\Omega_{\rm cdm}$
σ_8
w_0

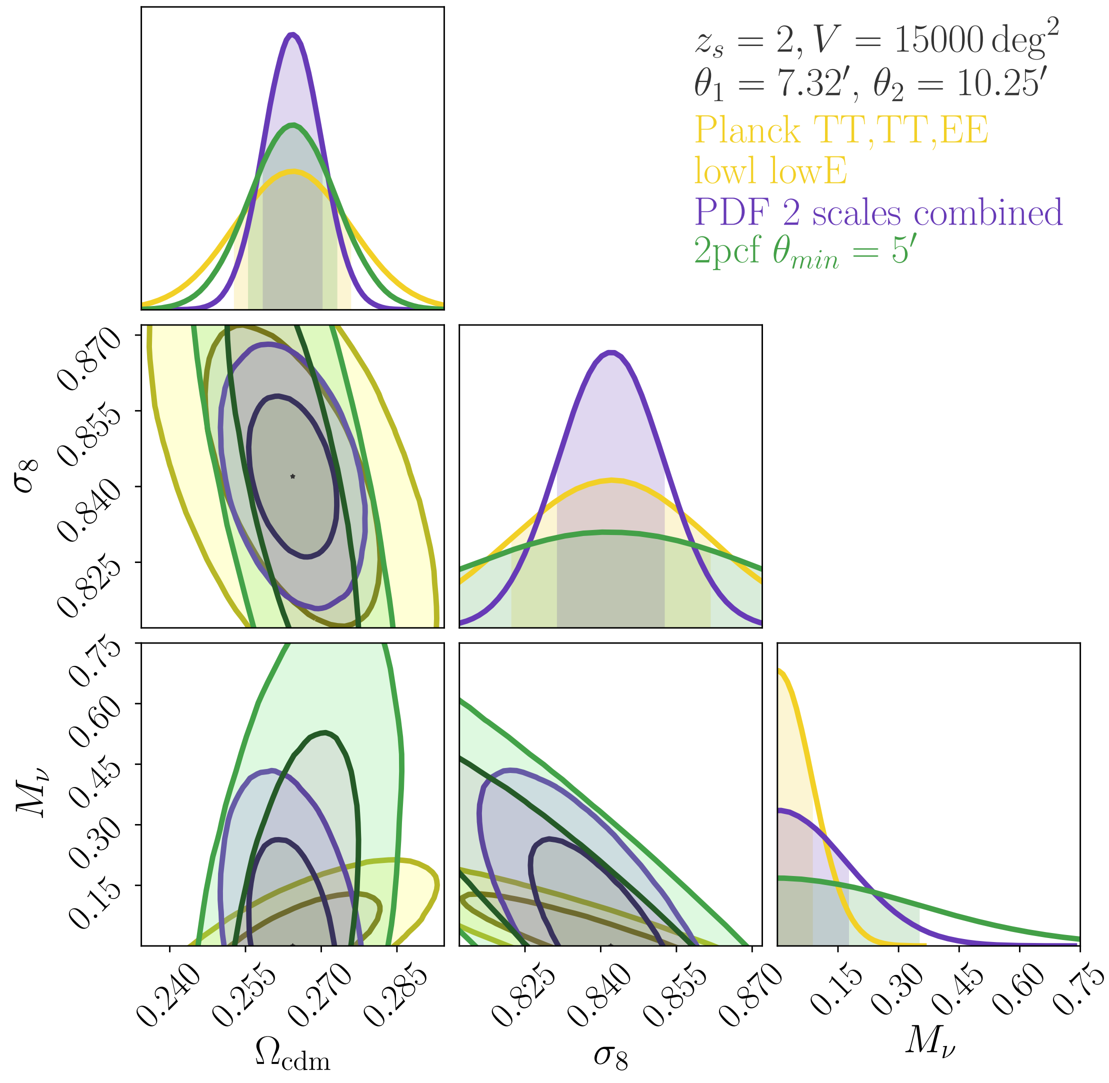
$z_s = 2, V = 15000\,\mathrm{deg}^2$
$\theta_1 = 7.32', \theta_2 = 10.25'$
Planck TT,TT,EE
lowl lowE
PDF 2 scales combined
2pcf $\theta_{min} = 5'$
σ_8
M_ν
$\Omega_{\rm cdm}$
σ_8
M_ν

Extended Results

Planck+PDF vs. Planck	ΛCDM	ΛCDM+M_ν	wCDM
$\Omega_{\rm cdm}$	+55%	+43%	+65%
σ_8	+43%	+40%	79%
$\Omega_{\rm b}$	+52%	+37%	+67%
n_s	+25%	+24%	+20%
h	+53%	+39%	+74%
M_ν (eV)	-	+31%	-
w_0	-	-	+78%
Planck+PDF vs. Planck+2pcf	**ΛCDM**	**ΛCDM+M_ν**	**wCDM**
$\Omega_{\rm cdm}$	0%	+23%	+36%
σ_8	+8%	+32%	+35%
$\Omega_{\rm b}$	+0%	+26%	+37%
n_s	+0%	+2%	+4%
h	+0%	+25%	+36%
M_ν (eV)	-	+27%	-
w_0	-	-	+40%

Ω_b, n_s, h added in using only theoretical derivatives.

More conservative shape noise parameters adopted here (8 gal arcmin^{-2}).

Significant improvements in constraints on σ_8, M_ν, w_0 when using PDF over correlation function!

Preliminary result for Planck + PDF + 2pcf: 50% improvements for extended cosmologies (15% for σ_8 in ΛCDM).

Conclusions (Part 2)

- Model of Barthelemy et al. (2020) captures cosmology dependence very accurately, allowing for robust calculations of Fisher derivatives.
- Accurate non-linear variances can be obtained from Halofit and accurate covariance matrices can be produced with fast simulation codes like FLASK. Therefore, forecasts like these can be performed without any reliance on N-body/ray-tracing simulations.
- The region of the PDF we probe has a Gaussian likelihood, unlike the first few moments.
- The PDF outperforms the 2-point correlation function in cosmological constraining power.
- Our theoretical model has allowed us to perform the first forecast for the WL PDF that varies the full set of LCDM parameters.

Future Work

- Extend to multiple source redshifts, which Liu & Madhavacheril (2018) found helped significantly improve constraints.

Thank you!

(1) NLO Nuisance Derivatives

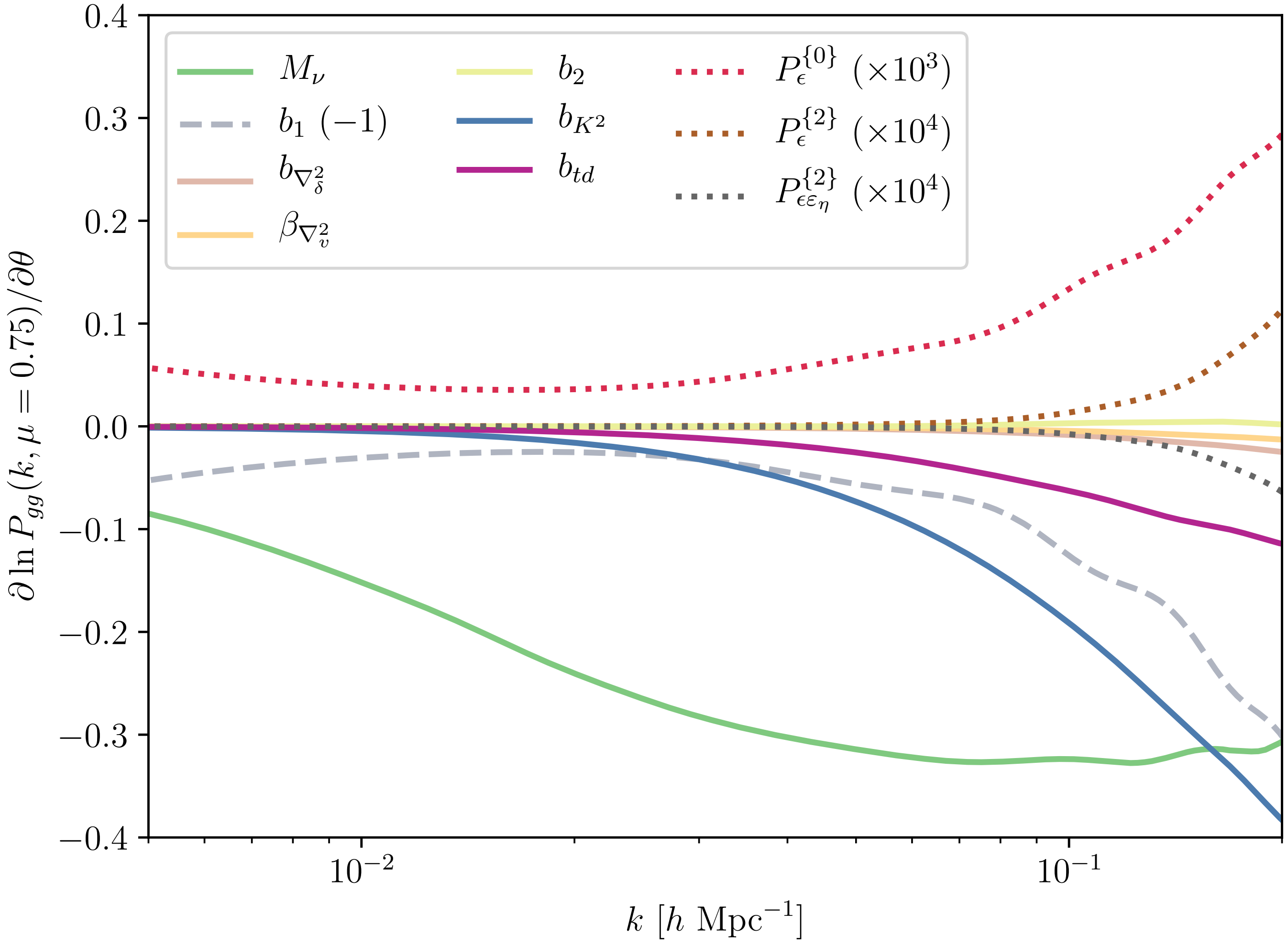

(2) Simulation Issues

Nulling technique uses linear combinations of maps for different source redshifts to 'null' small scales.

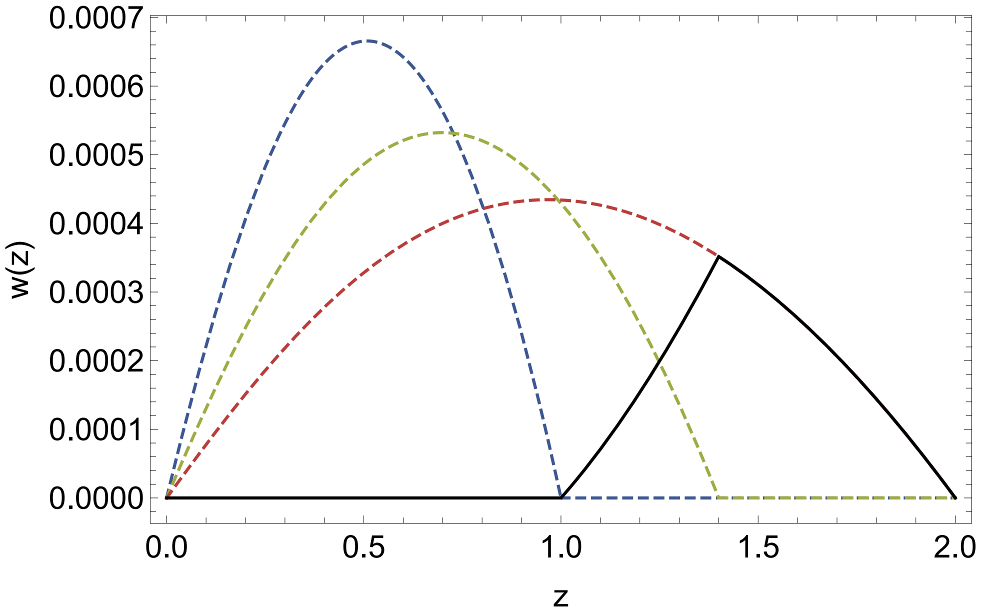

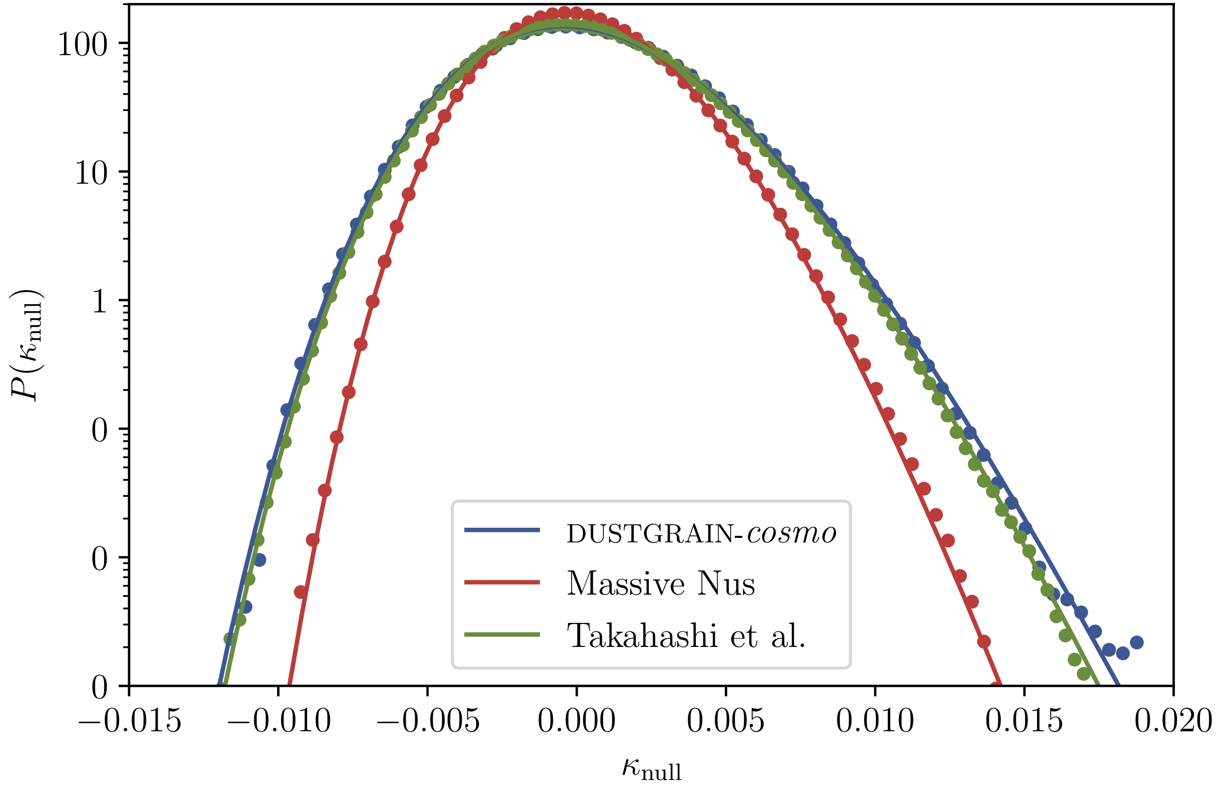

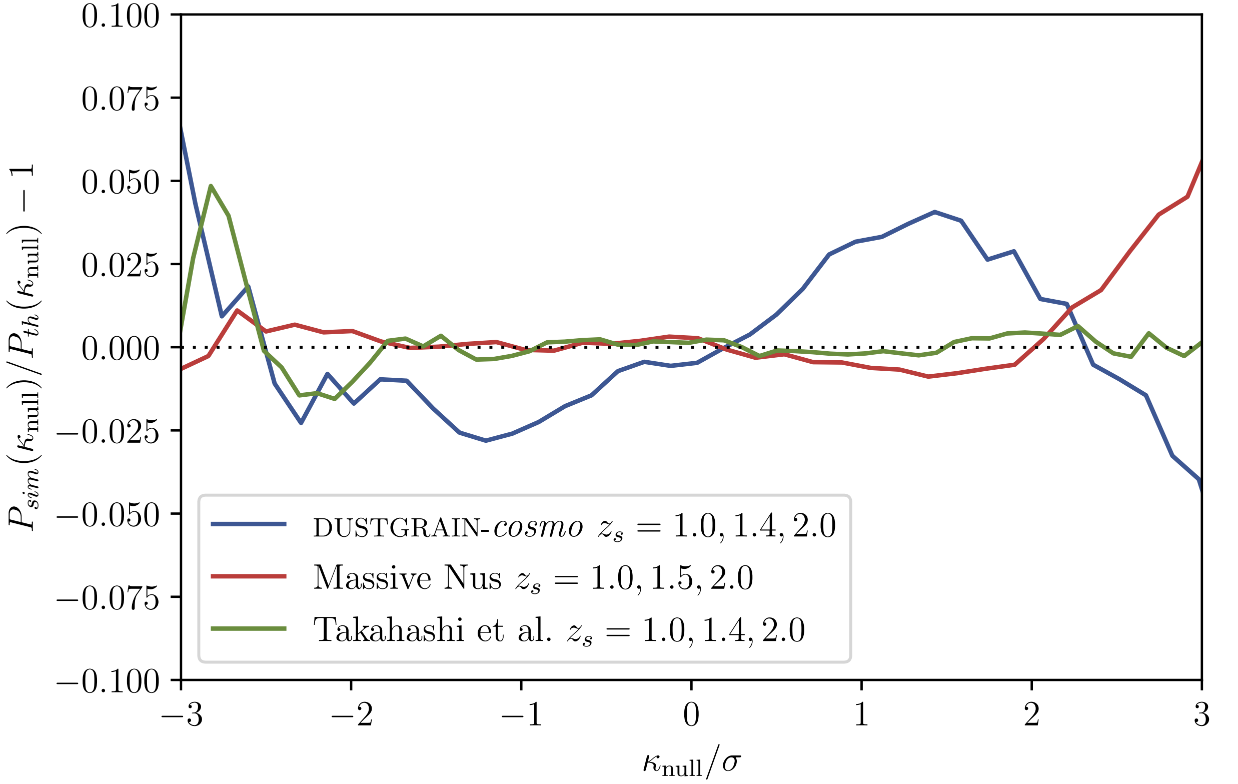

(2) Patch Size Issues

Difficulties replicating 2-point correlation function with Halofit for smaller maps, even when introducing cut in *l*.

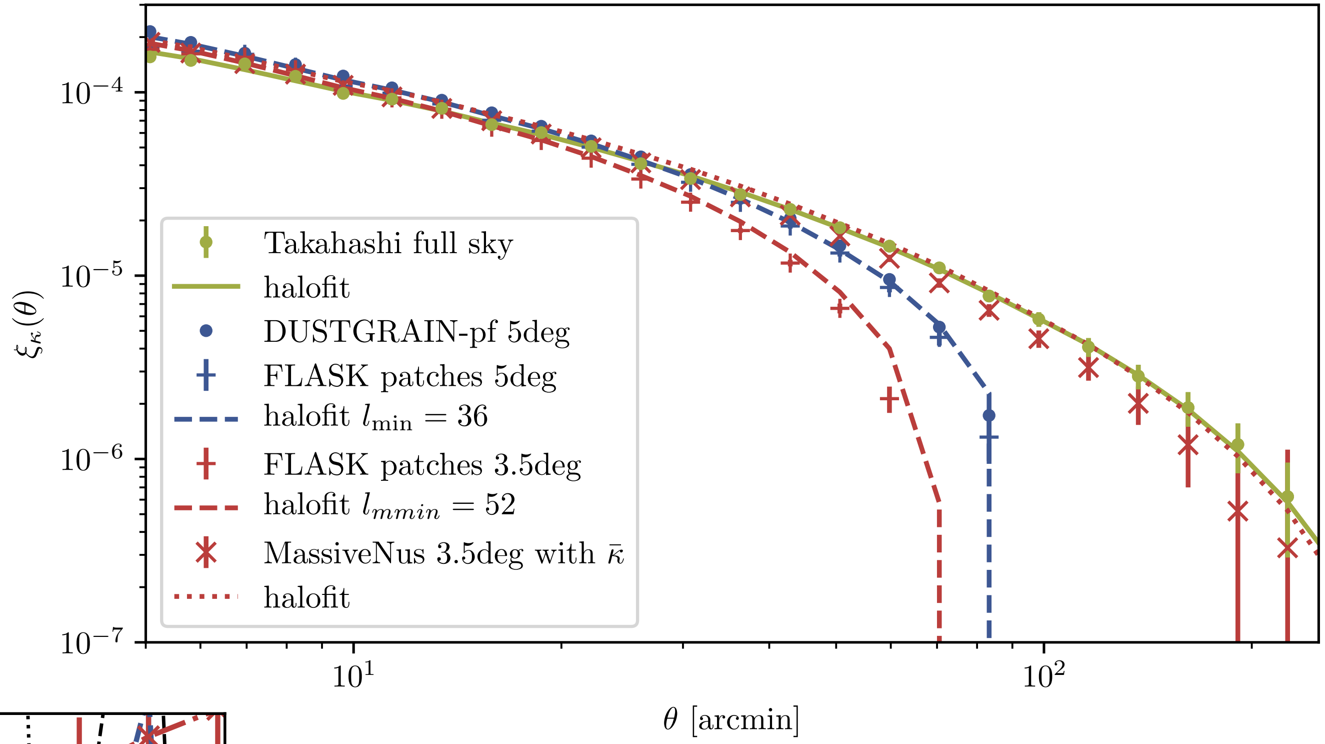

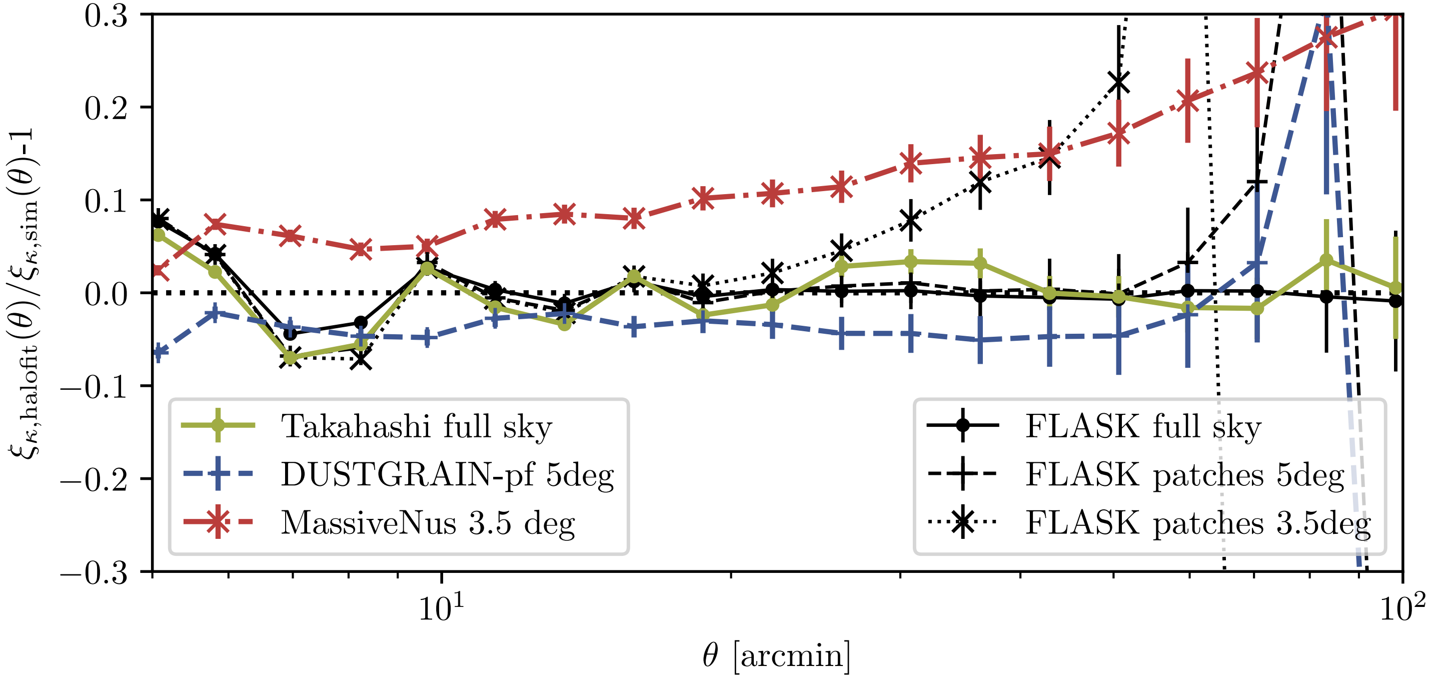

Aoife Boyle

(2) LDT in Cylinders

Rate function:

$$\Psi_{cyl}(\rho) = \frac{\boldsymbol{\delta_L^2(\rho)}}{2\sigma_L^2(z, \boldsymbol{r_{initial}(R,\rho)})} \frac{\boldsymbol{\sigma_L^2}}{\boldsymbol{\sigma_{NL}^2}}$$

Mass conservation: $r_{initial} = d_A \theta \rho^{\frac{1}{2}}$

Spherical collapse: Gives linear overdensity δ_L corresponding to final density ρ.

Approximately: $\delta_L(\rho) = \nu\left(1 - \rho^{-\frac{1}{\nu}}\right)$

ν is set to 1.4 to replicate PT tree-order skewness for cylindrical symmetry.

Non-linear variance provided by Halofit.

LDT predicts the *scaled* CGF

$$\varphi(y) = \lim_{\sigma^2 \to 0} \sigma^2 \phi\left(\frac{y}{\sigma^2}\right),$$

which is obtained as a Legendre transform of the rate function

$$\varphi(y) = y\delta - \frac{\sigma_L^2(D\theta, L, z)}{2\sigma_L^2\left(D\theta\sqrt{\rho}, L, z\right)} \delta_L^2(\rho).$$

We finally rescale the CGF ϕ with the correct variance

$$\phi(y) = \frac{\sigma_L^2}{\sigma_{NL}^2} \phi\left(\frac{\sigma_{NL}^2}{\sigma_L^2} y\right).$$

The PDF is obtained from the CGF with an inverse Laplace transform

$$P(\kappa) = \int_{-i\infty}^{i\infty} \frac{dy}{2\pi i} \exp(-y\kappa + \phi(y)).$$

(2) Third Cumulant

$$k_3^\kappa = \int_0^{z_s} R'(z)\omega^3(z,z_s)k_3^{cyl}(d_A(z)\theta, L, z)L^2$$